USTC - Particle and Nuclear Physics

NPMW Mini Workshop

Nuclear Structure Effect in Light-Ion Collisions

Xinli Zhao (赵新丽)

University of Shanghai for Science and Technology

12/08/2024, USTC, Hefei

In Collaboration with:

Guoliang Ma (马国亮), You Zhou (周铀), Ziwei Lin (林子威)

Deformed and Odd-shaped Atomic Nuclei

Deformations

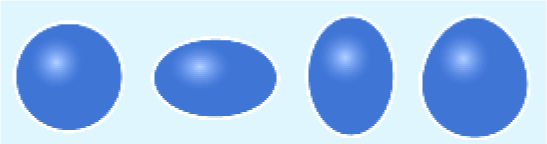

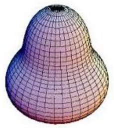

Odd-shaped

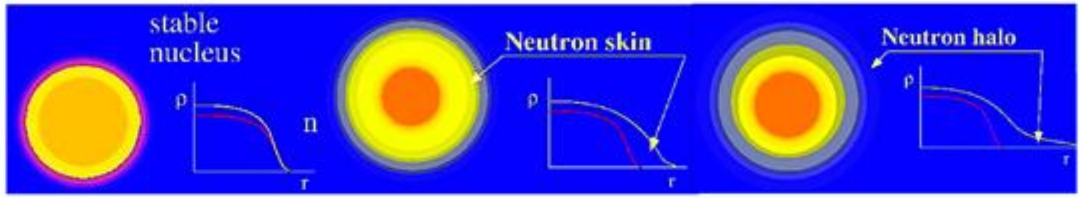

Deformed and Odd-shaped Atomic Nuclei

Deformations

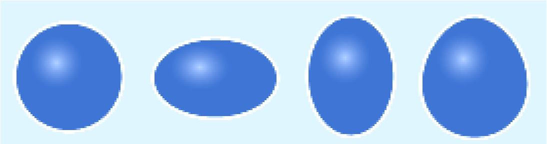

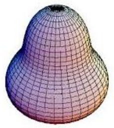

Odd-shaped

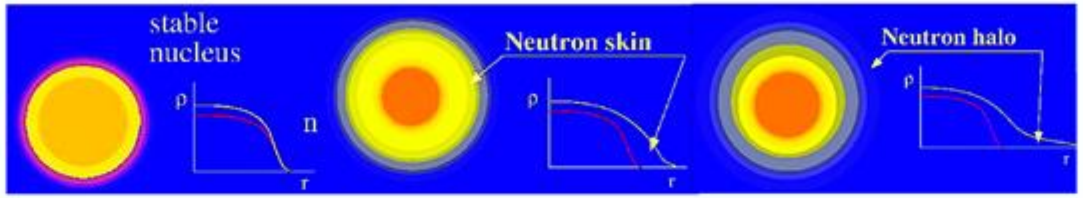

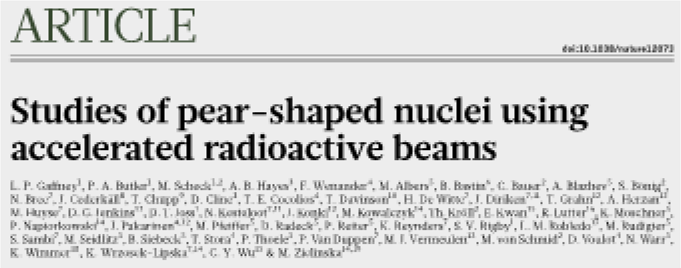

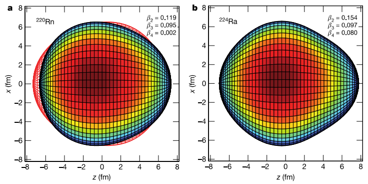

Deformed and Odd-shaped Atomic Nuclei

Deformations

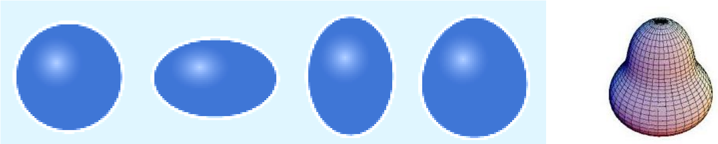

Odd-shaped

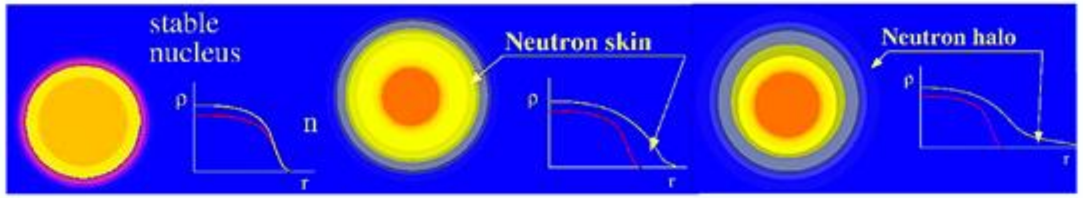

ARTICLE

Studies of pear-shaped nuclei using accelerated radioactive beams

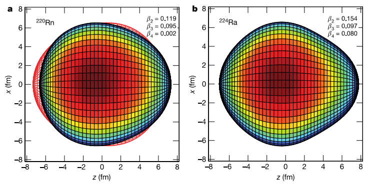

Article

Imaging shapes of atomic nuclei in high-energy nuclear collisions

C.J. Zhang, J.Y. Jia, et al., Nature 635, 67 (2024)

https://doi.org/10.1038/s41586-024-08097-2 STAR Collaboration*

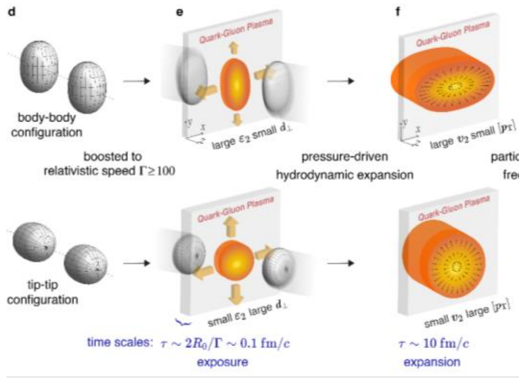

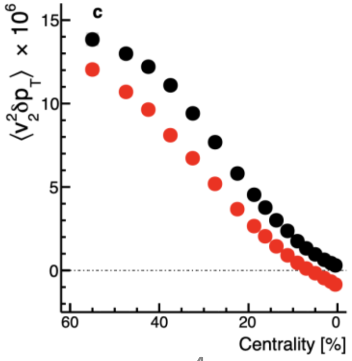

Deformed and Odd-shaped Atomic Nuclei

Deformations

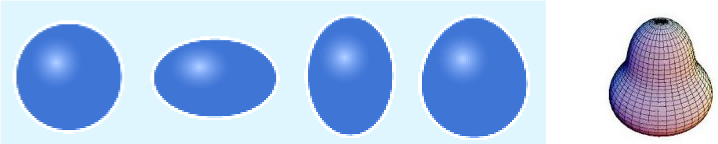

Odd-shaped

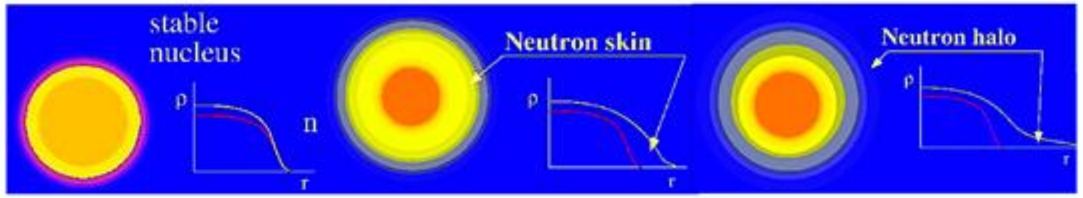

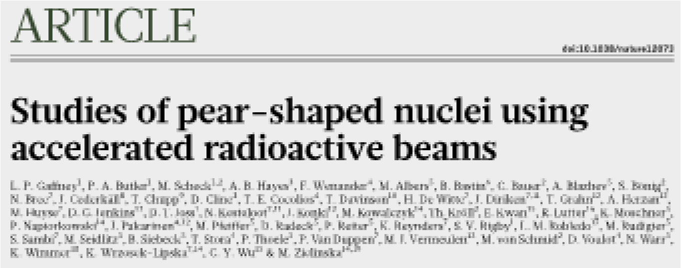

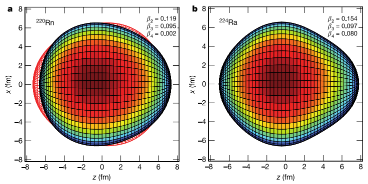

$$\rho(r,\theta,\phi) = \frac{\rho_0}{1 + e^{(r - R(\theta,\phi))/a_0}}$$

$$R(\theta,\phi) = R_0(1 + \beta_2[\cos\gamma Y_{2,0}(\theta,\phi) + \sin\gamma Y_{2,2}(\theta,\phi)] + \beta_3 Y_{3,0}(\theta,\phi) + \beta_4 Y_{4,0}(\theta,\phi))$$

Quadrupole

Octupole

Hexadecapole

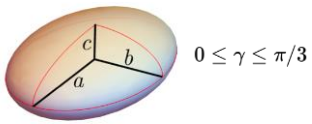

Prolate: a=b<c à β_2, γ=0

Oblate: a<b=c à β_2, γ=π/3

Triaxial: a<b<c à β_2, γ=π/6

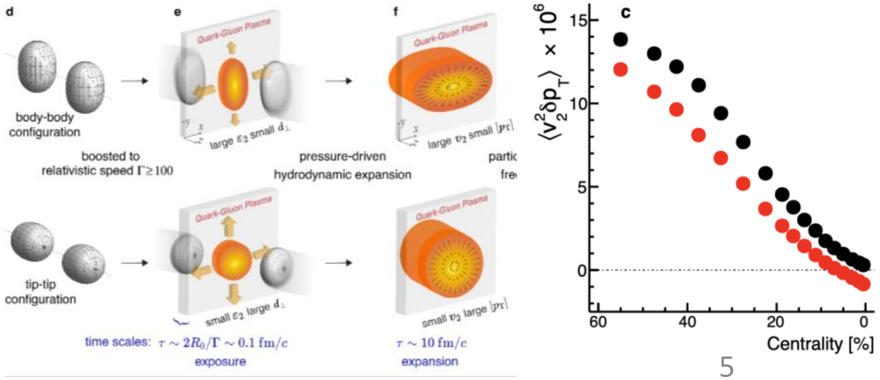

➢ The study of nuclear structure in high-energy heavy ion collisions uniquely reveals how nuclear properties affect collision dynamics and QGP formation.

Cluster Structures

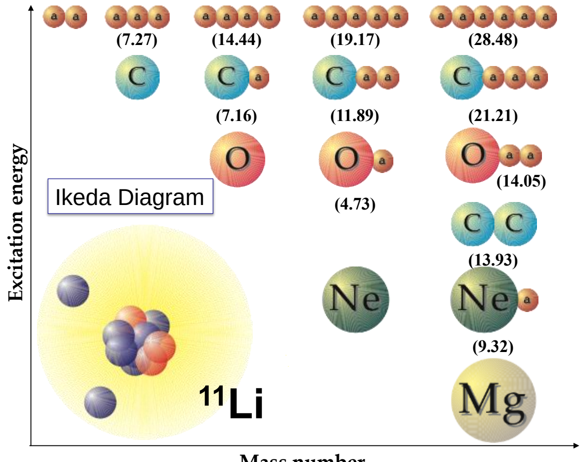

http://www.nndc.bnl.gov/qcalc/

sequence of reaction channels

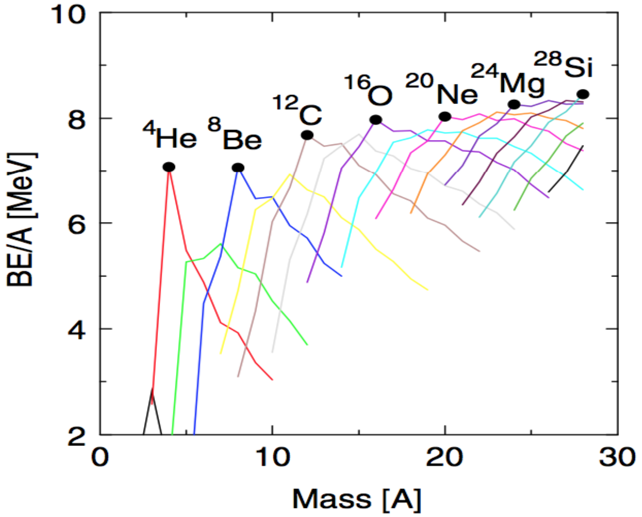

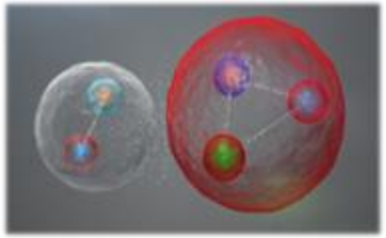

5-quark cluster

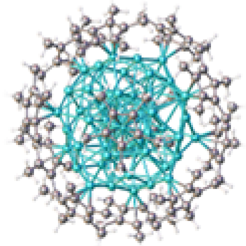

Multi-atom cluster

Galaxy cluster

Cluster Structures

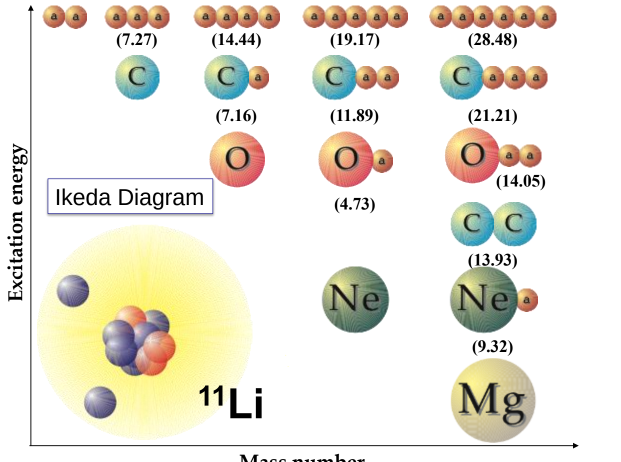

http://www.nndc.bnl.gov/qcalc/

sequence of reaction channels

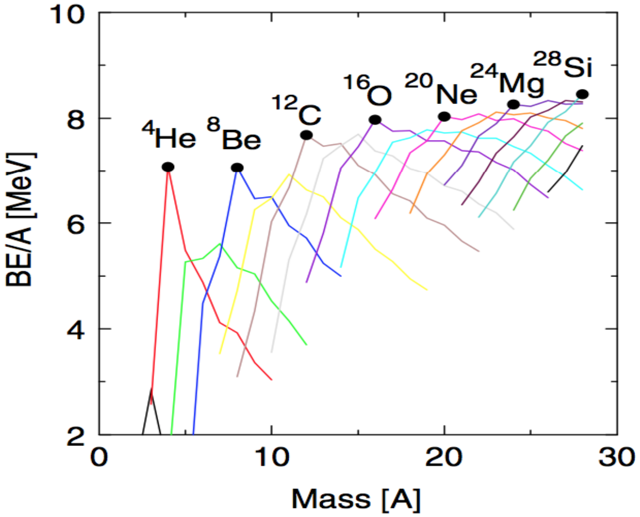

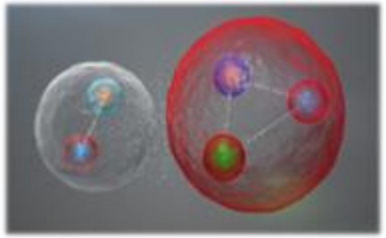

5-quark cluster

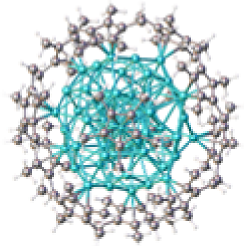

Multi-atom cluster

Galaxy cluster

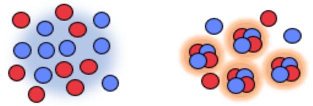

Nucleosynthesis in astrophysics

During the nuclear excitation, phase transitions occur then form nuclear clusters.

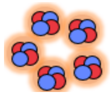

Nuclear excitation

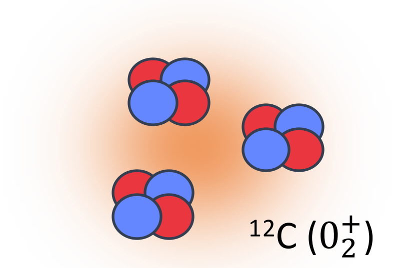

3α Bose-Einstein condensate

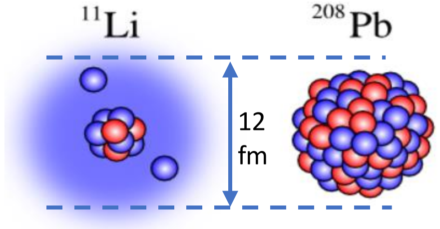

Halo type for ^{11}Li

- ➢ Clusters play an extremely important role at all levels of matter.
- ➢ Understanding and describing cluster structure are an important scientific problem.

Cluster Structures

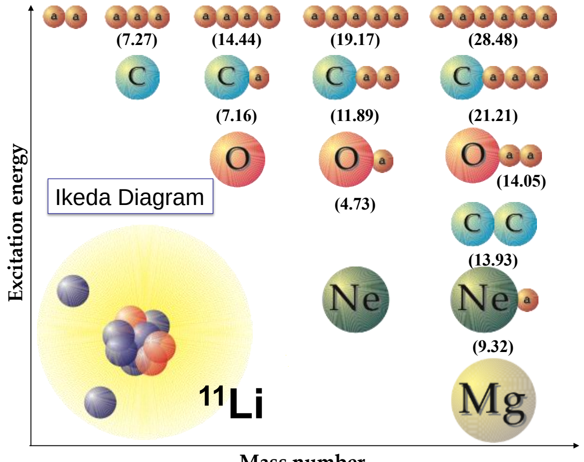

http://www.nndc.bnl.gov/qcalc/

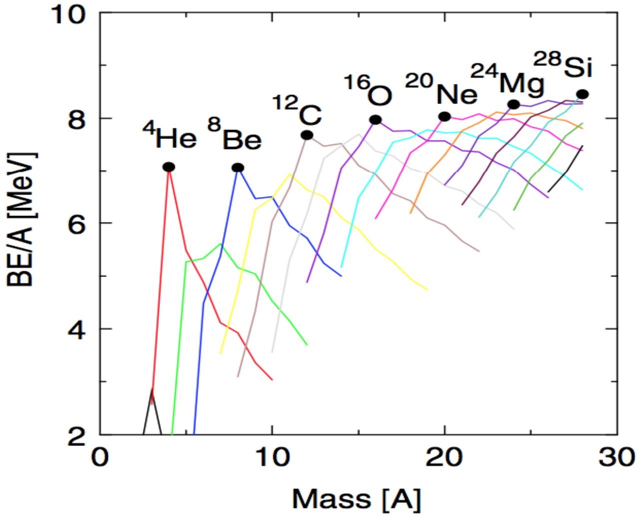

sequence of reaction channels

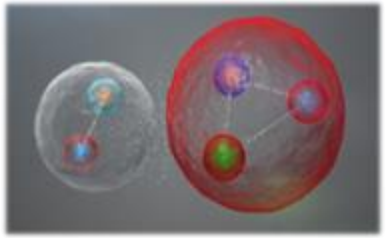

5-quark cluster

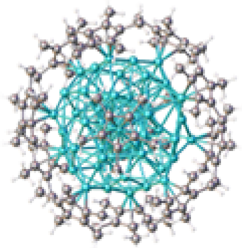

Multi-atom cluster

Galaxy cluster

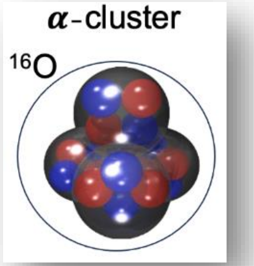

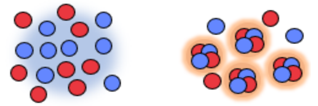

Nucleosynthesis in astrophysics

During the nuclear excitation, phase transitions occur then form nuclear clusters.

Nuclear excitation

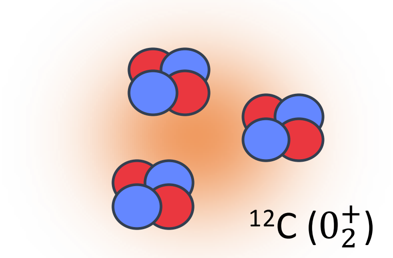

3α Bose-Einstein condensate

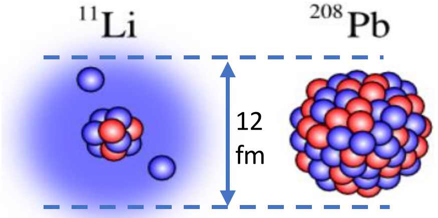

Halo type for ^{11}Li

nucleonic clustering

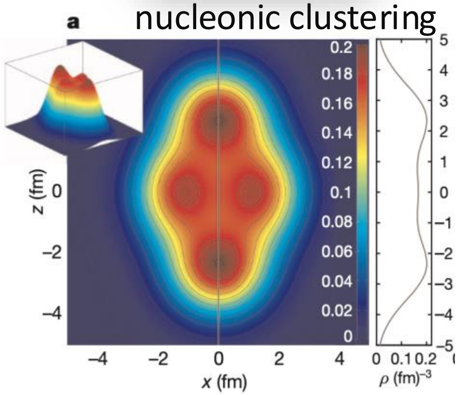

^{20}Ne

J.P. Ebran et al. Nature487, 341(2012)

- Clusters play an extremely important role at all levels of matter.
- Understanding and describing cluster structure are an important scientific problem.

Collective Flow & Nuclear Structure

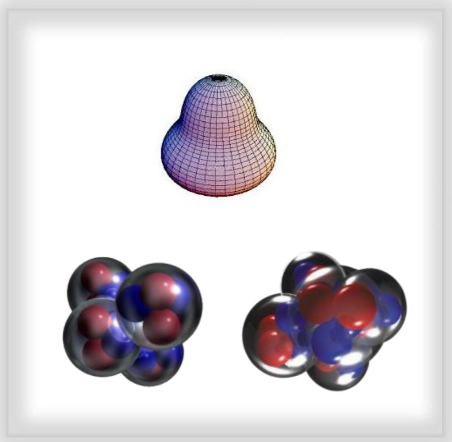

$$\frac{\rho_0}{1+e^{(r-R_0(1+\sum_n \beta_n Y_n^0(\theta,\phi))/a_0}}$$

Initial size   Initial shape

$R_\perp^2 \propto \langle r_\perp^2 \rangle$ $\mathcal{E}_n \propto \langle r_\perp^n e^{in\phi} \rangle$

R_0 a_0 β_n

From J.Y. Jia's talk

imaging

Initial Geometry

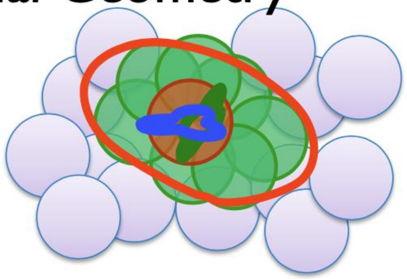

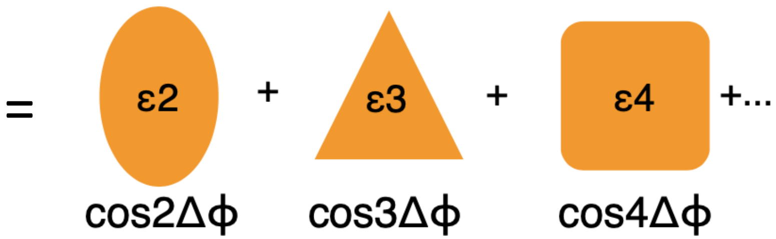

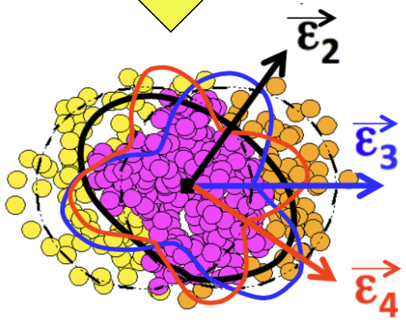

Hydro-response

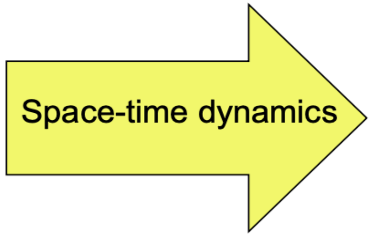

Particle distribution

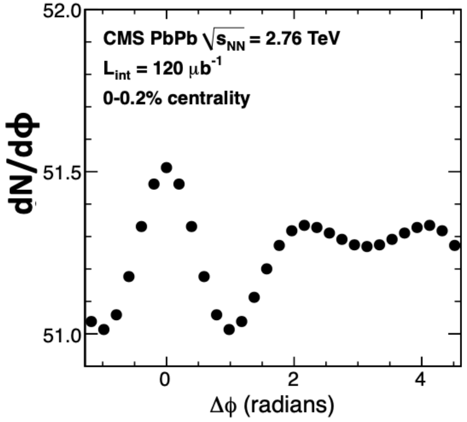

Approximate linear response: $\frac{\delta[p_T]}{[p_T]} \propto -\frac{\delta R_\perp}{R_\perp}$ $V_n \propto \mathcal{E}_n$

➢ Image the shape and radial profile of nuclei using the hydrodynamic response.

Motivation of Transport Models for Small Systems

Pb + Pb

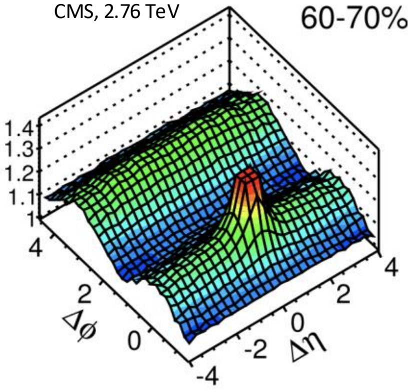

CMS, EPJC (2012) 72:2012

***p* + Pb**

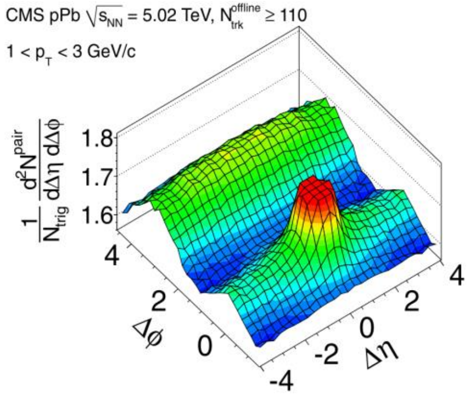

CMS, PLB 718 (2013) 795–814

p* + *p

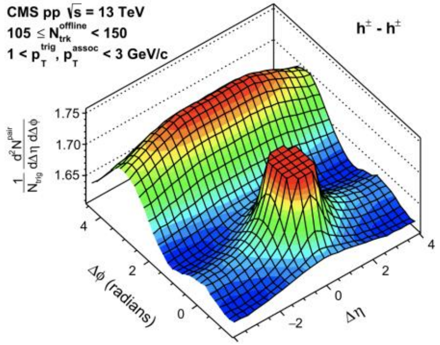

CMS, PLB 765 (2017) 193–220

Large systems

Small systems

- Near side ridges are indication of collectivity in small systems.

1) Are they real signals from collectivity?
2) Is a parton matter formed in small systems?
3) Is the matter far off equilibrium or close to equilibrium?

Motivation of Transport Models for Small Systems

Pb + Pb

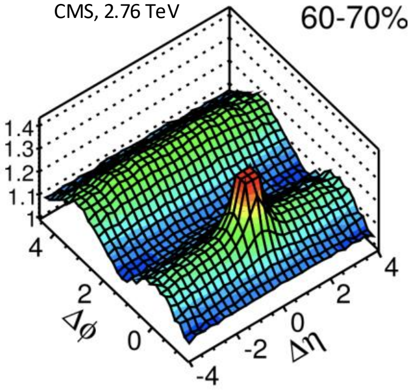

CMS, EPJC (2012) 72:2012

$p + \mathrm{Pb}$

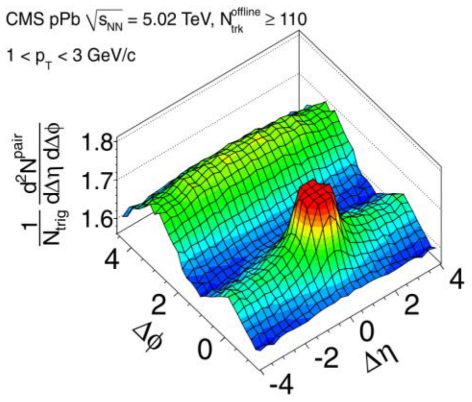

CMS, PLB 718 (2013) 795–814

$p + p$

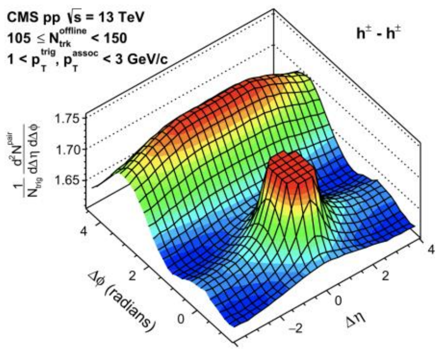

CMS, PLB 765 (2017) 193–220

Large systems → Small systems

Pb+Pb	O+O	p+A
U+U	Ne+Ne	d+A
Au+Au	Ca+Ca	He+A
Xe+Xe	…	…

- ➢ Near side ridges are indication of collectivity in small systems.
1) Are they real signals from collectivity?
2) Is a parton matter formed in small systems?
3) Is the matter far off equilibrium or close to equilibrium?

- ➢ **For large systems**
- ✓ Transport models are similar to hydrodynamics and work very well.
- ➢ **2) For finite/small systems**
- ✓ Non-equilibrium effects are expected to be important.
- ✓ *e.g.* Parton escape mechanism: interaction-induced response from kinetic theory to the anisotropic spatial geometry.

➢ To study the properties of parton matter in small systems, transport models are crucial as they address non-equilibrium dynamics.

A Multi-Phase Transport Model (AMPT)

- A transport model for non-equilibrium.
- AMPT is designed to be a self-contained kinetic description of nuclear collisions.

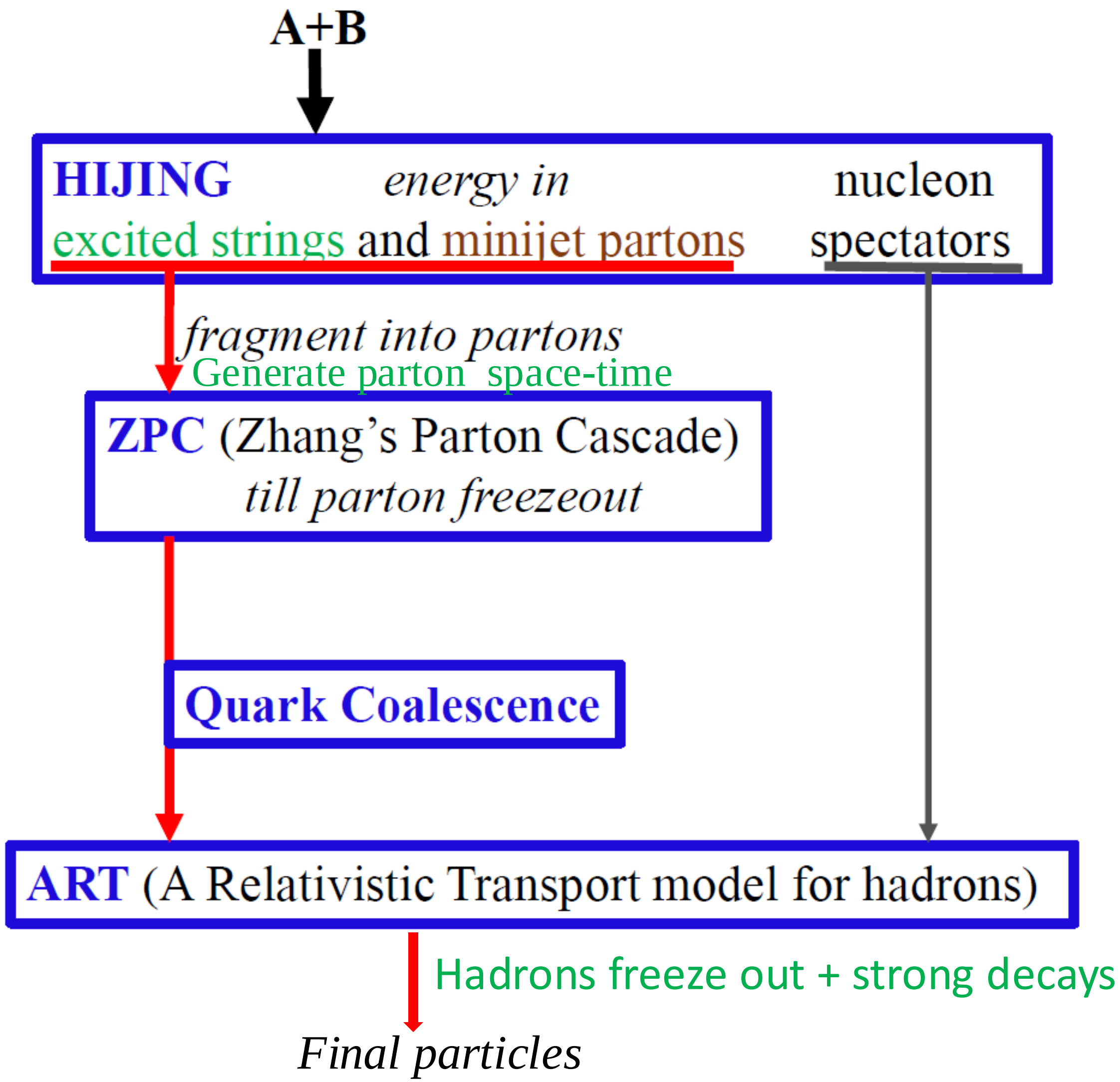

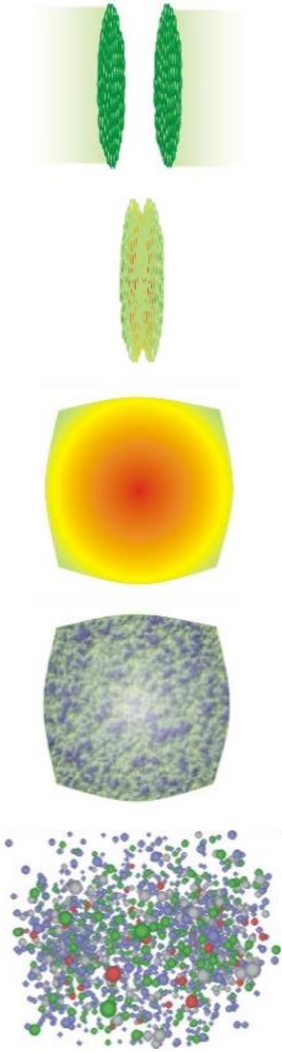

Z.W. Lin, Phys. Rev. C 72 (2005) 064901.

A Multi-Phase Transport Model (AMPT)

- A transport model for non-equilibrium.
- AMPT is designed to be a self-contained kinetic description of nuclear collisions.
- Evolves the system from initial state to final observables.
- Automatically includes 3D productions of all flavours & conserved charges.
- Automatically includes non-equilibrium initial state & dynamics/evolution.

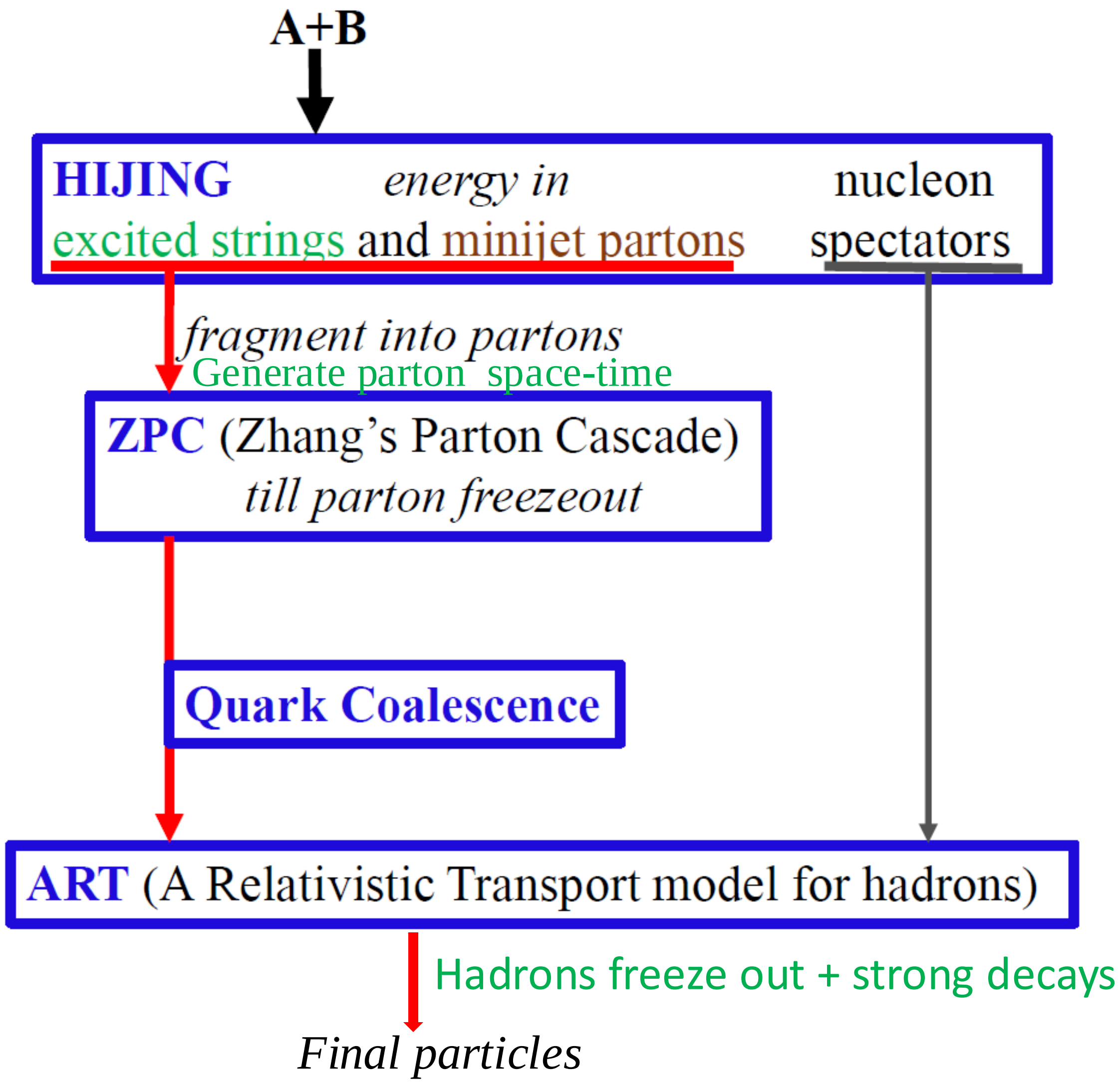

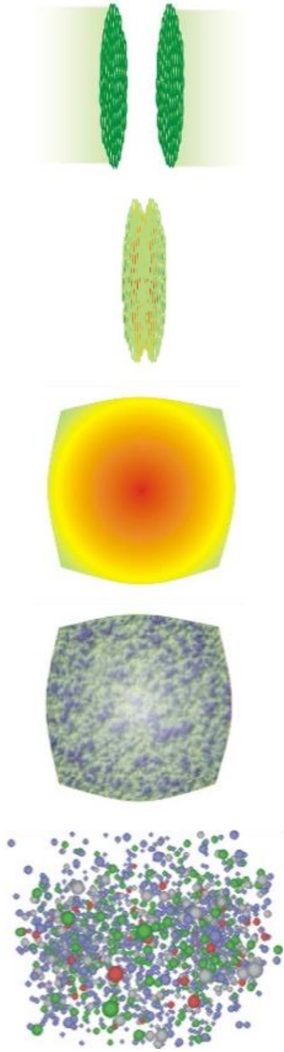

Z.W. Lin, Phys. Rev. C 72 (2005) 064901.

A Multi-Phase Transport Model (AMPT)

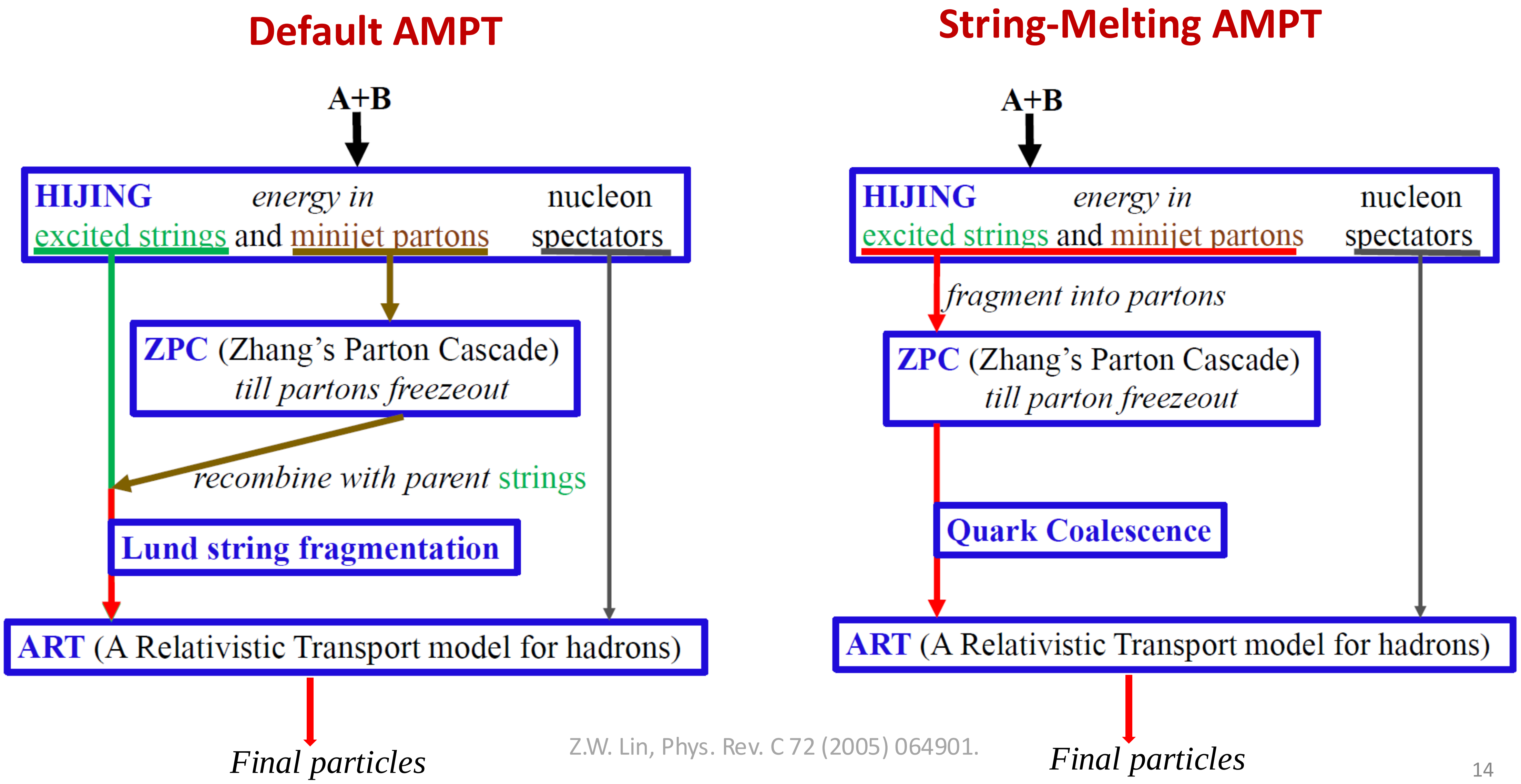

Z.W. Lin, Phys. Rev. C 72 (2005) 064901.

A Multi-Phase Transport Model (AMPT)

Default AMPT

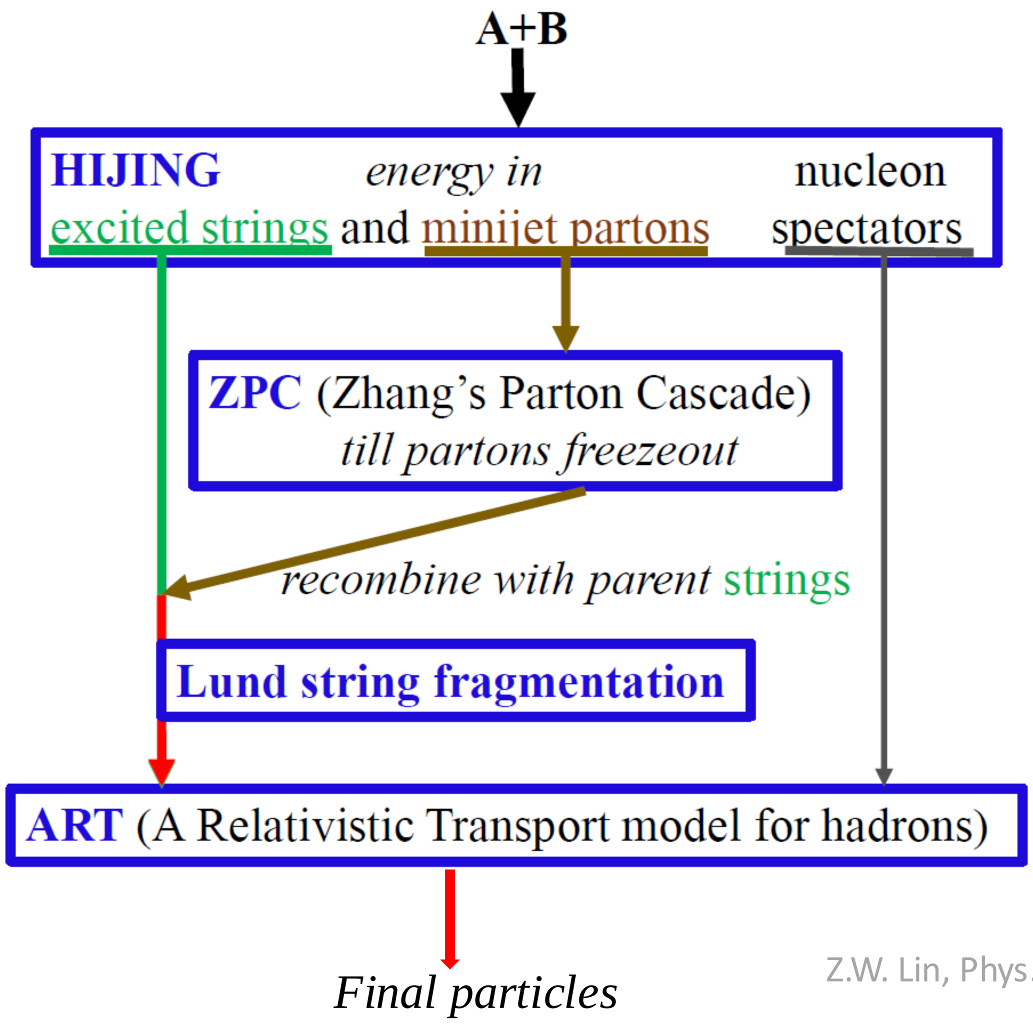

String-Melting AMPT

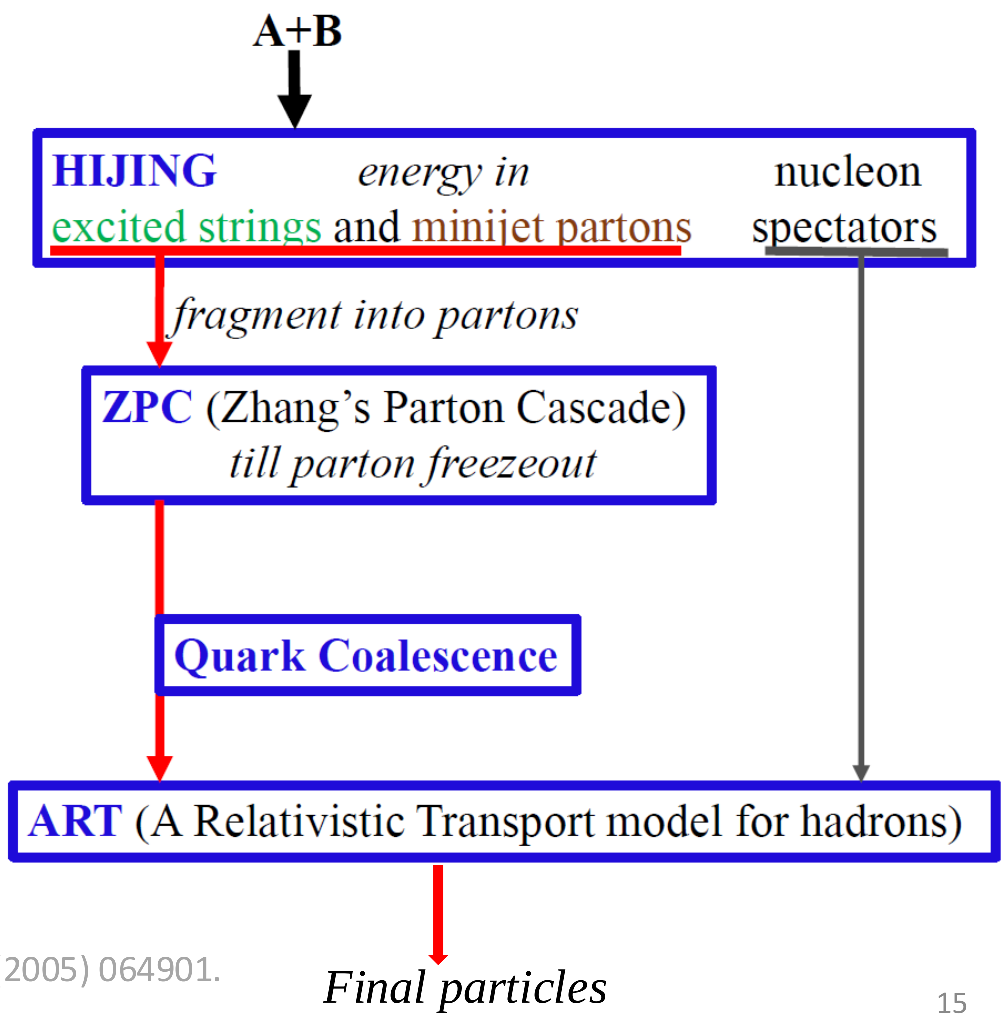

Z.W. Lin, Phys. Rev. C 72 (2005) 064901.

A Test-bed for New Ideas in AMPT

1. Discovery of v_3

PRC 81, 054905 (2010)

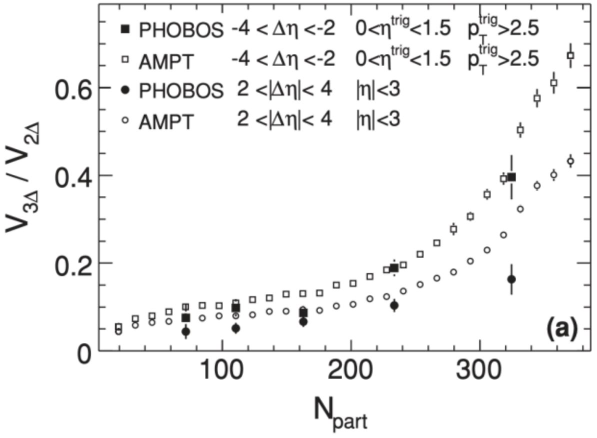

2. Flow in small systems

PRL 113, 252301 (2014)

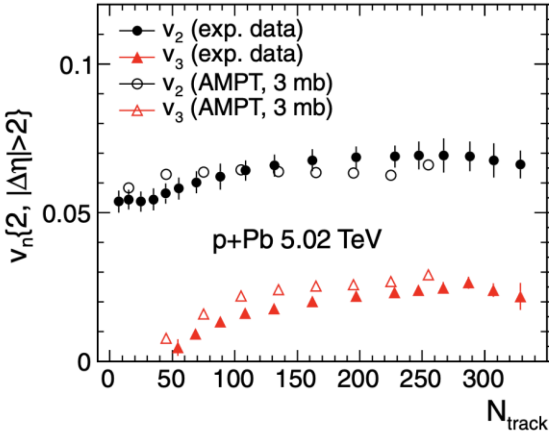

3.Non-equilibrium parton escape

PLB 753 (2016) 506–510

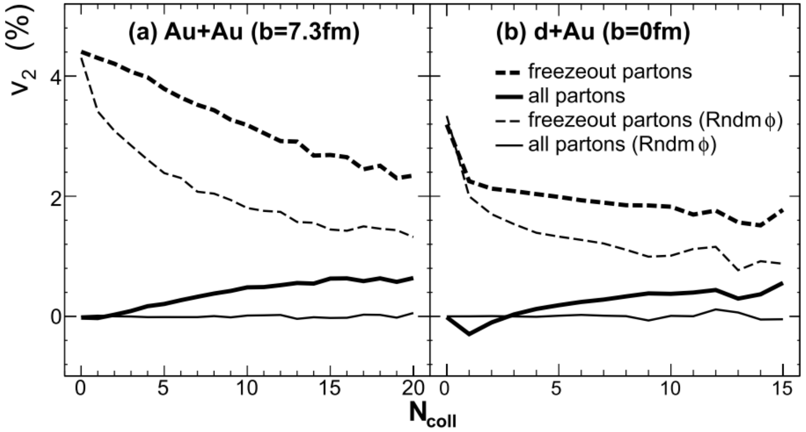

4. Longitudinal decorrelations

PRC 91, 044904 (2015)

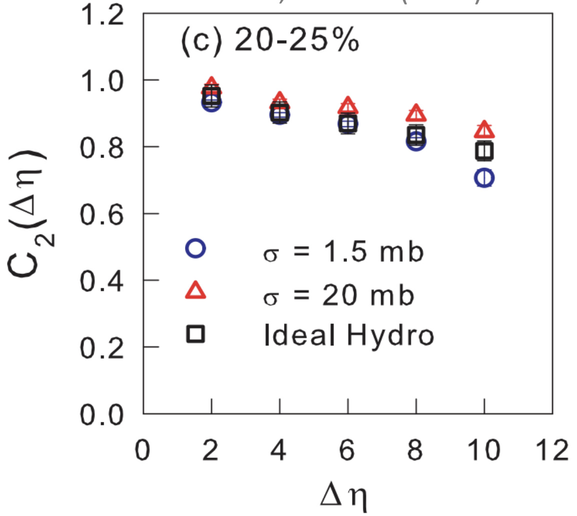

5. Effects of nuclear structure

J.Y. Jia, G. Giacalone, et al., 2404.08385

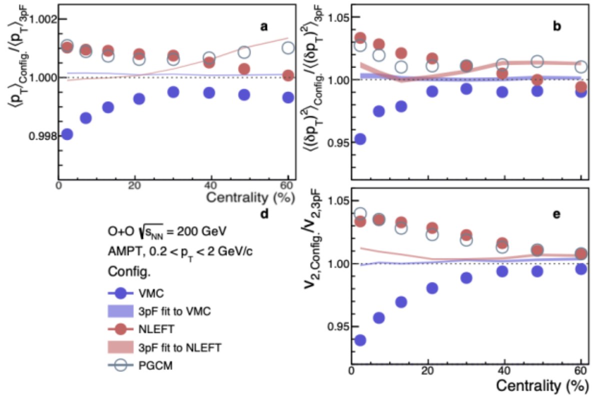

J.Y. Jia, G. Giacalone, and C.J. Zhang, PRL 121, 022301 (2018)

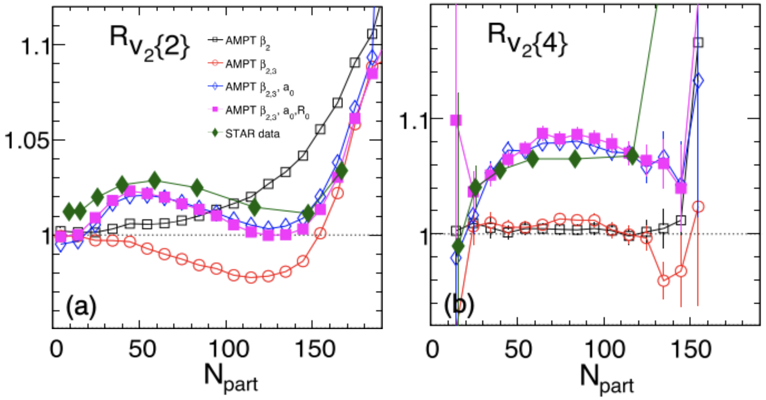

S.L. Huang, et al., PRC **101**, 021901(R)

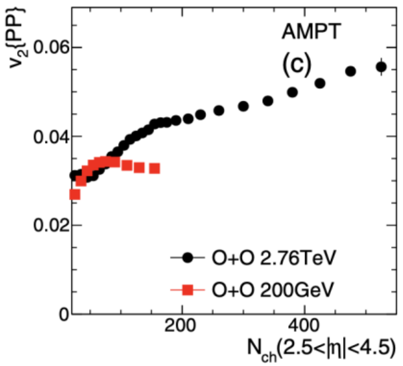

PRL 125, 222301 (2020) (Ru+Ru & Zr+Zr collisions)

PRC 103, 064906 (2021) (p+O/O+O collisions)

Some Major Improvements in AMPT

Z.W. Lin, et al., NUCL SCI TECH (2021) 32:113
Z.W. Lin, PRC 99 (2019); PRC 101 (2020)

1. Modern nPDFs & spatially-dependent nuclear shadowing

- ✓ Modern nPDFs are important for pQCD observables such as heavy flavor & high p_T:

$$\frac{d\sigma^{Q\bar{Q}}}{dp_T^2 dy_1 dy_2} = K \sum_{a,b} x_1 f_a(x_1, \mu_F^2) x_2 f_b(x_2, \mu_F^2) \frac{d\sigma^{ab \to Q\bar{Q}}}{d\hat{t}}$$

nPDFs for the free nucleon

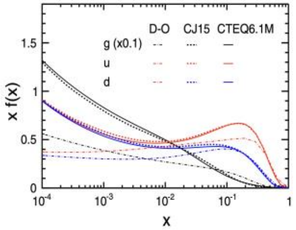

EPS09s nuclear shadowing

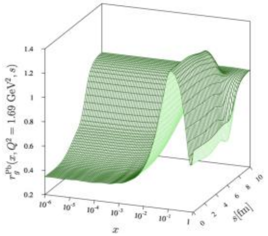

- ✓ Introducing A-scaling for central AA

$$\sigma_{\rm jet} = \sum_{c,d} \frac{1}{1+\delta_{cd}} \int_{p_0^2}^{s/4} dp_T^2 dy_1 dy_2 \frac{d\sigma^{cd}}{dp_T^2 dy_1 dy_2} \qquad p_0^{AA} = p_0^{pp} A^{q(s)}$$

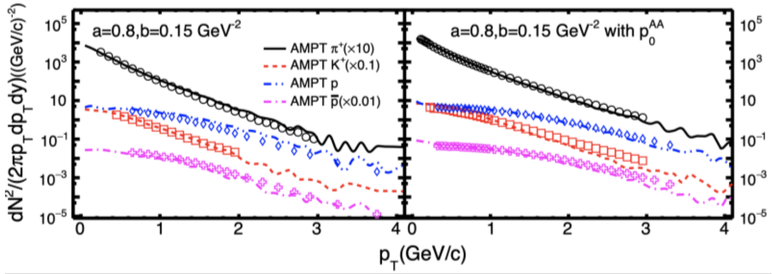

➢ AMPT can reasonably describe central A+A data.

Some Major Improvements in AMPT

Z.W. Lin, et al., NUCL SCI TECH (2021) 32:113
Z.W. Lin, PRC 99 (2019); PRC 101 (2020)

1. Modern nPDFs & spatially-dependent nuclear shadowing

✓ Modern nPDFs are important for pQCD observables such as heavy flavor & high p_T:

$$\frac{d\sigma^{Q\bar{Q}}}{dp_T^2 dy_1 dy_2} = K \sum_{a,b} x_1 f_a(x_1,\mu_F^2) x_2 f_b(x_2,\mu_F^2) \frac{d\sigma^{ab\to Q\bar{Q}}}{d\hat{t}}$$

nPDFs for the free nucleon

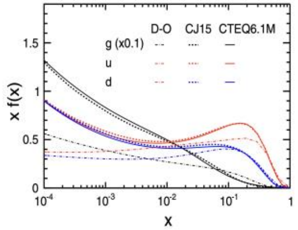

EPS09s nuclear shadowing

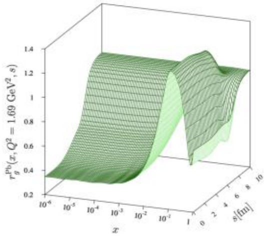

✓ Introducing A-scaling for central AA

$$\sigma_{\rm jet} = \sum_{c,d} \frac{1}{1+\delta_{cd}} \int_{p_0^2}^{s/4} dp_T^2 dy_1 dy_2 \frac{d\sigma^{cd}}{dp_T^2 dy_1 dy_2} \quad p_0^{AA} = p_0^{pp} A^{q(s)}$$

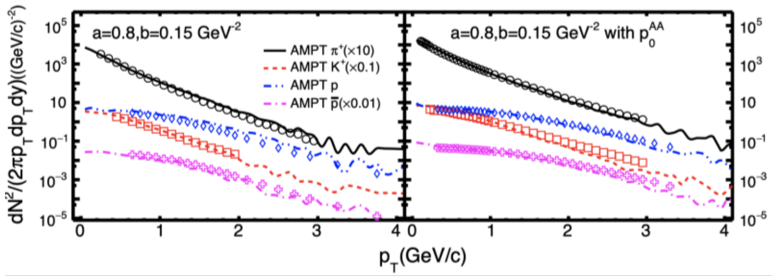

➢ AMPT can reasonably describe central A+A data.

2. Heavy flavor

$gg \to gg$ cross section in pQCD is divergent for massless g, so HIJING uses a minijet cutoff p_0:

$$\frac{d\sigma}{dt} \sim \frac{9\pi\alpha_s^2}{2t^2}$$

But due to heavy quark mass, heavy flavor production has a finite cross section and does not need a cutoff

$$g + g \to Q + \bar{Q}, \quad q + \bar{q} \to Q + \bar{Q}, \ \ldots$$

✓ remove p_0

✓ include heavy ion in σ_{jet}: $\sigma_{jet} = \sigma_{jet}^{LF} + \sigma^{HF}$

✓ correct factor of 1/2 in certain σ_{jet} channels

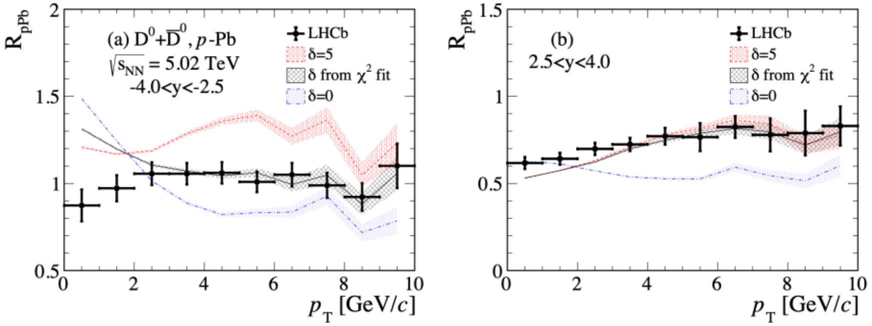

➢ To propose the Cronin effect as a possible solution to the D_0 $R_{\rm pA}/v_2$ puzzle.

Some Major Improvements in AMPT

3. Local nuclear scaling

C Zhang, Z.W. Lin, et al., PRC 104 (2021)

- ✓ Propose a more general scaling by using local nuclear densities:

$$b_L(s_A, s_B, s) = \frac{b_L^{pp}}{[\sqrt{T_A(s_A)T_B(s_B)}/T_p]^{\beta(s)}}$$

$$p_0(s_A, s_B, s) = p_0^{pp}(s)[\sqrt{T_A(s_A)T_B(s_B)}/T_p]^{\alpha(s)}$$

- ✓ Fit charged hadrons in *pp* to determine $b_L^{pp} = 0.7$, then use central Au+Au/Pb+Pb data to fit $\alpha(s)$, $\beta(s)$.

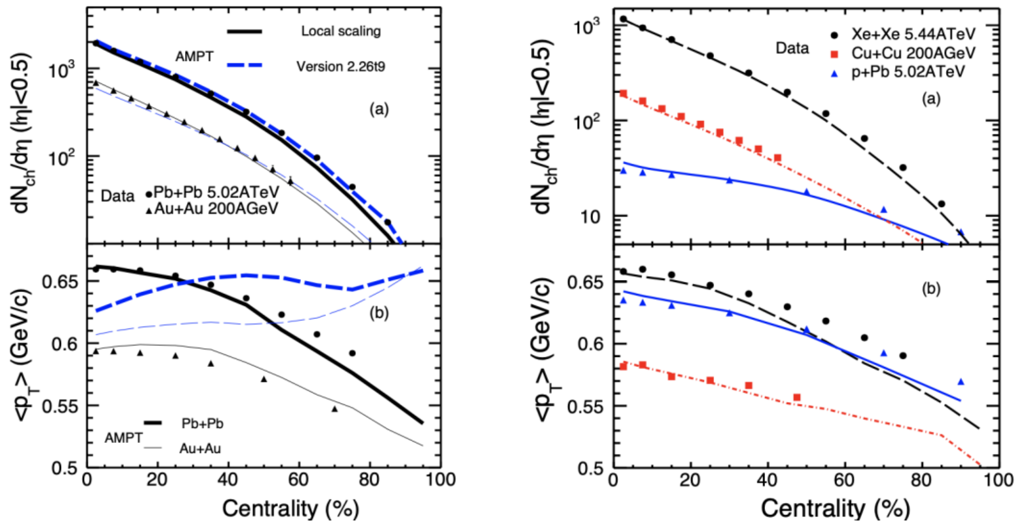

➢ Self-consistently describe the system size dependence.

Some Major Improvements in AMPT

3. Local nuclear scaling

C Zhang, Z.W. Lin, et al., PRC 104 (2021)

✓ Propose a more general scaling by using local nuclear densities:

$$b_L(s_A, s_B, s) = \frac{b_L^{pp}}{[\sqrt{T_A(s_A)T_B(s_B)}/T_p]^{\beta(s)}}$$

$$p_0(s_A, s_B, s) = p_0^{pp}(s)[\sqrt{T_A(s_A)T_B(s_B)}/T_p]^{\alpha(s)}$$

✓ Fit charged hadrons in *pp* to determine $b_L^{pp} = 0.7$, then use central Au+Au/Pb+Pb data to fit $\alpha(s)$, $\beta(s)$.

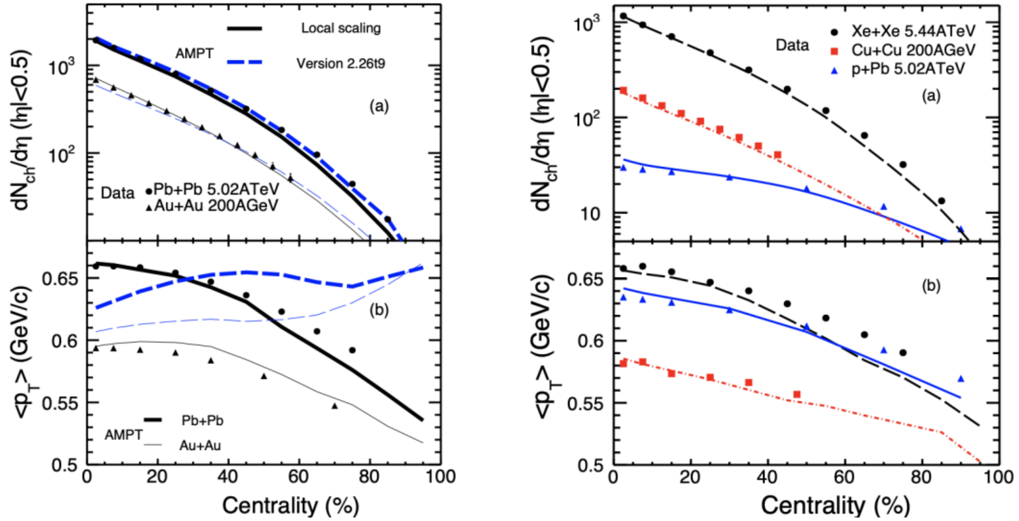

➢ Self-consistently describe the system size dependence.

4. Include subnucleon structure of proton

✓ Proton substructure

$$\rho(r) = \frac{1}{8\pi R^3} e^{-r/R}$$

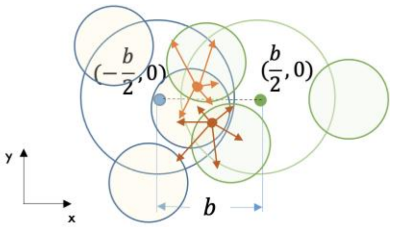

✓ Constituent quark method

Glauber modeling with 3 quark participants

Collision criteria $d < \sqrt{\sigma_{cc}/\pi}$

XL Zhao, ZWL, L Zheng & GL Ma, PLB 839 (2023)

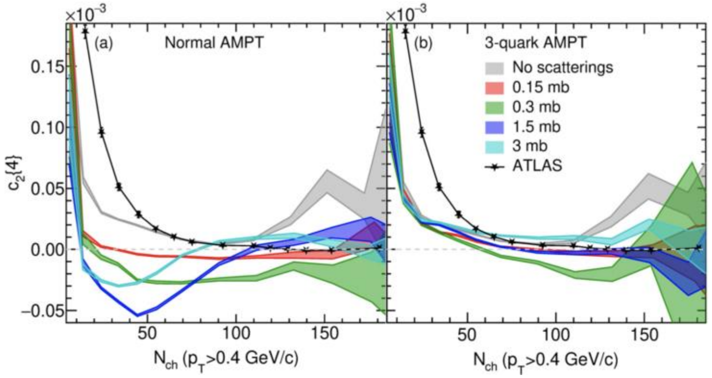

➢ 3-quark AMPT gives similar results as data.

Some Major Improvements in AMPT

3. Local nuclear scaling

C Zhang, Z.W. Lin, et al., PRC 104 (2021)

- ✓ Propose a more general scaling by using local nuclear densities:

$$b_L(s_A, s_B, s) = \frac{b_L^{pp}}{[\sqrt{T_A(s_A)T_B(s_B)}/T_p]^{\beta(s)}}$$

$$p_0(s_A, s_B, s) = p_0^{pp}(s)[\sqrt{T_A(s_A)T_B(s_B)}/T_p]^{\alpha(s)}$$

- ✓ Fit charged hadrons in *pp* to determine $b_L^{pp} = 0.7$, then use central Au+Au/Pb+Pb data to fit $\alpha(s)$, $\beta(s)$.

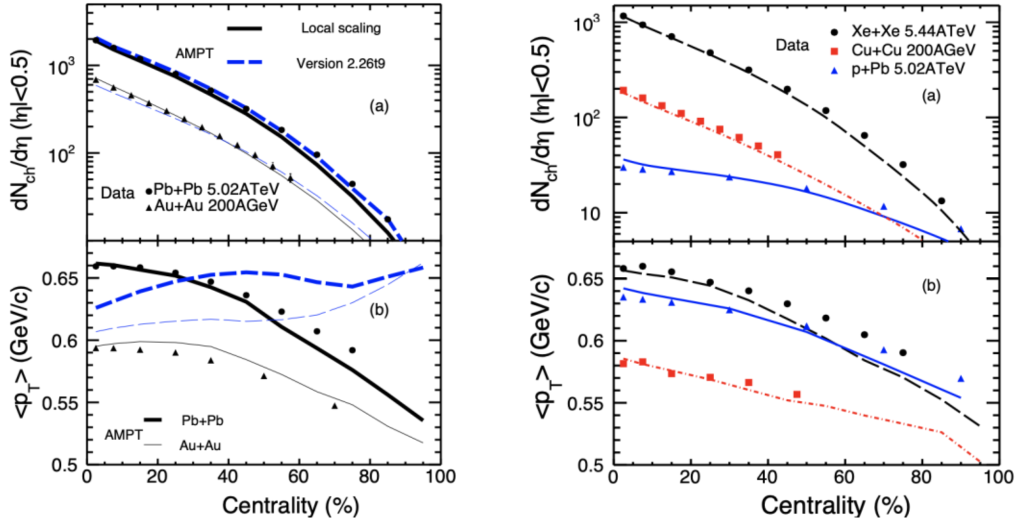

➤ Self-consistently describe the system size dependence.

4. Include subnucleon structure of proton

- ✓ Proton substructure

$$\rho(r) = \frac{1}{8\pi R^3} e^{-r/R}$$

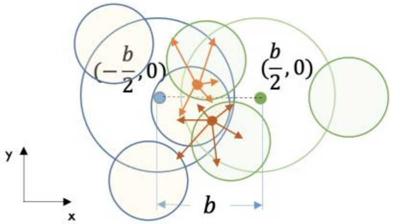

- ✓ Constituent quark method

Glauber modeling with 3 quark participants

Collision criteria $d < \sqrt{\sigma_{cc}/\pi}$

XL Zhao, ZWL, L Zheng & GL Ma, PLB 839 (2023)

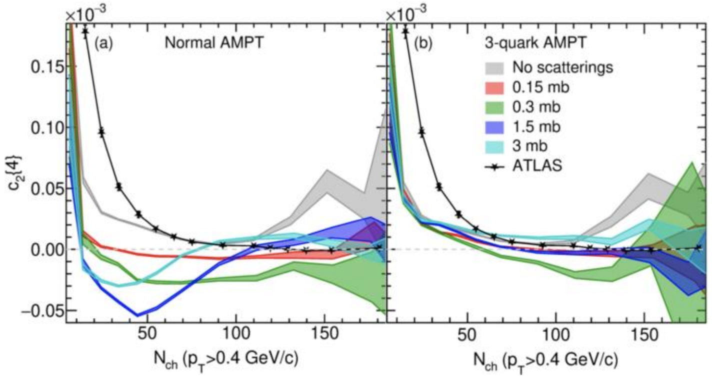

➤ 3-quark AMPT gives similar results as data.

5. Improvement of quark coalescence
6. Implementation of electric charge conservation
7. …

Nuclear Structure for ^{16}O in AMPT

1) New quark coalescence model
2) Improved heavy quark productions
3) Modern PDFs, nuclear shadowing and Local nuclear scaling

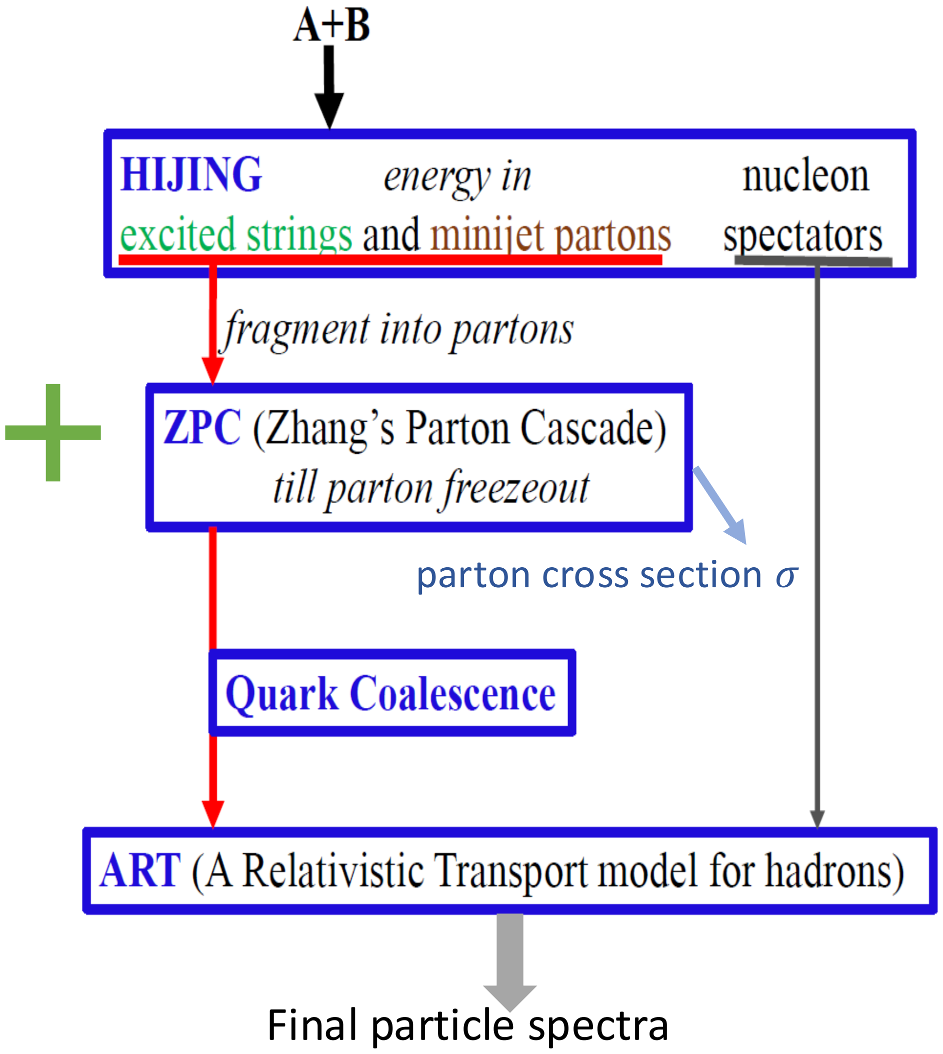

Nuclear Structure for ^{16}O in AMPT

A+B

HIJING *energy in* excited strings and minijet partons | nucleon spectators

fragment into partons

ZPC (Zhang's Parton Cascade) *till parton freezeout*

parton cross section σ

Quark Coalescence

ART (A Relativistic Transport model for hadrons)

Final particle spectra

1) New quark coalescence model
2) Improved heavy quark productions
3) Modern PDFs, nuclear shadowing and Local nuclear scaling

Constraint: $\langle r^2 \rangle^{1/2} = 2.6991 \text{ fm}$

1. Woods-Saxon

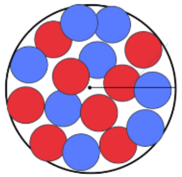

2. Tetrahedron

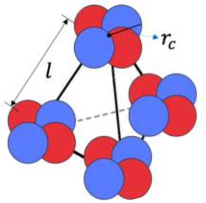

3. Square

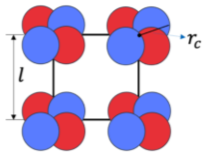

4. *ab initio* method (NLEFT)

N. Summerfield, B.-N. Lu, C. Plumberg, D. Lee, J. Noronha-Hostler, and A. Timmins, Phys. Rev. C 104, L041901 (2021), 2103.03345.

τ_0 Effect on v_2 for ^{16}O+^{16}O in Improved AMPT

X.L. Zhao, Y. Zhou, et al., arXiv: 2404.09780 cc

- $\langle p_T \rangle$ is reasonable in improved AMPT.
- The parton cross section dependence of v_2 is significant.

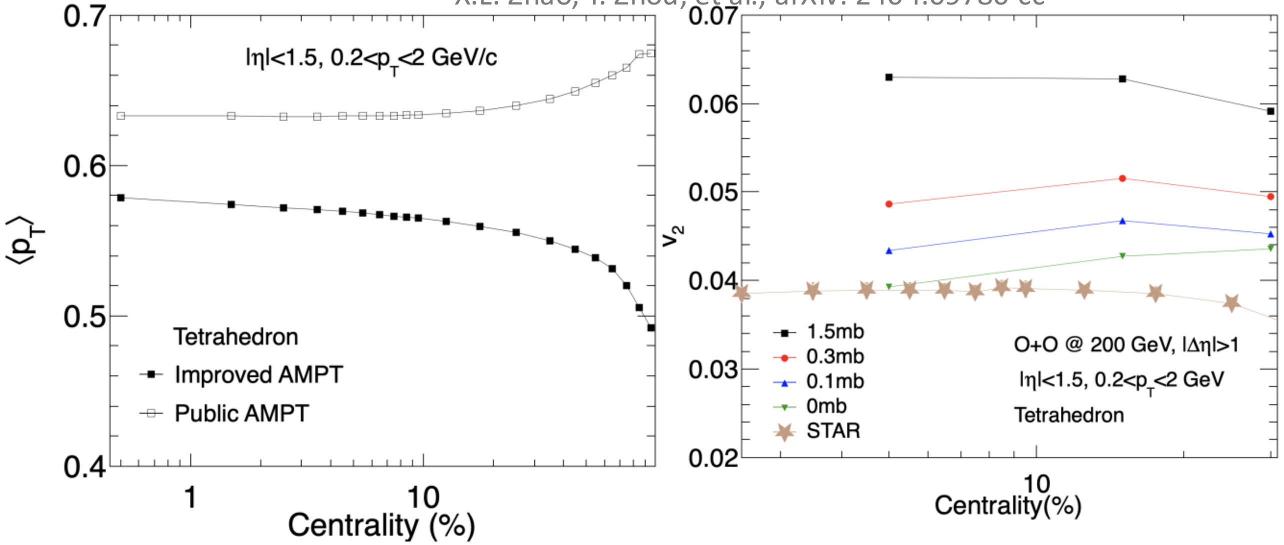

τ_0 Effect on v_2 for $^{16}O+^{16}O$ in Improved AMPT

X.L. Zhao, Y. Zhou, et al., arXiv: 2404.09780 cc

- $\langle p_T \rangle$ is reasonable in improved AMPT.
- The parton cross section dependence of v_2 is significant.

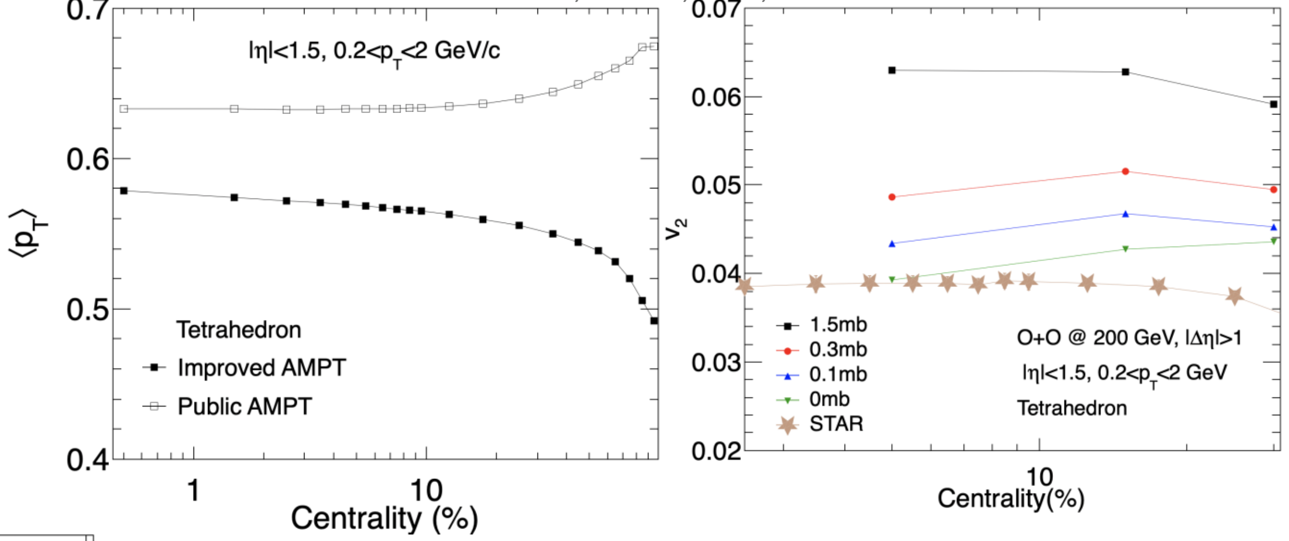

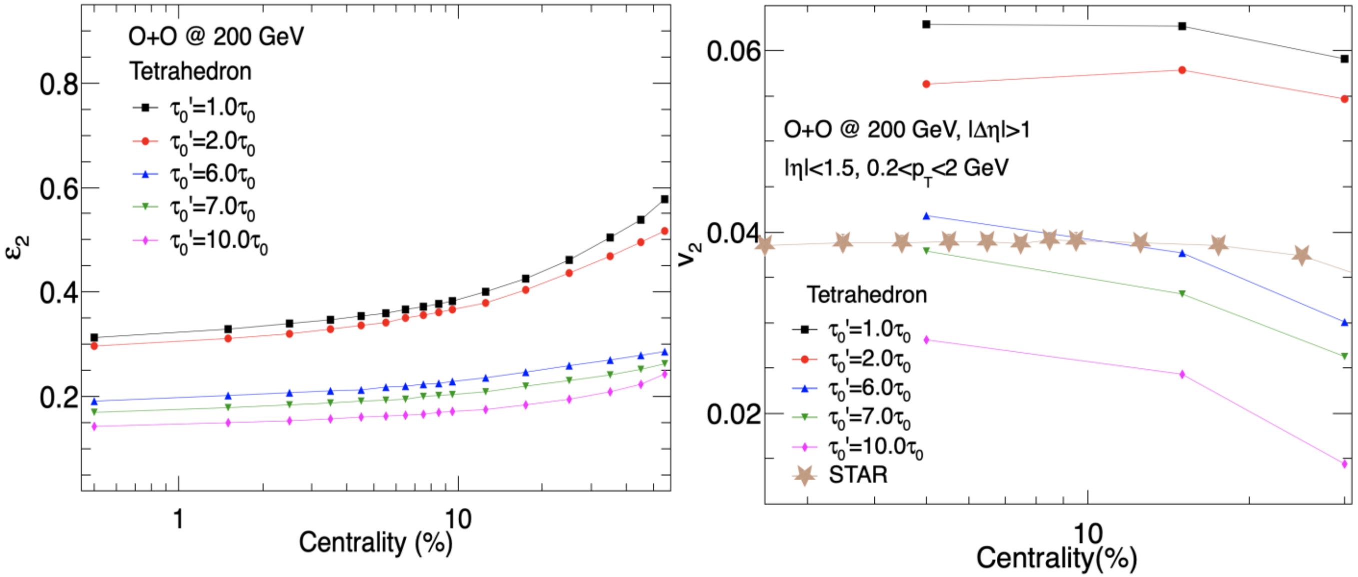

- The formation time dependence of ε_2 & v_2 is significant in AMPT.
- v_2 at $\tau_0' = 6\tau_0$ is close to data.

The formation time for each parton: $\tau_0' = const \cdot E/m_T^2,\ \tau_0 = E/m_T^2$

v_2 & v_3 Results for ^{16}O+ ^{16}O in Improved AMPT

X.L. Zhao, Y. Zhou, et al., arXiv: 2404.09780

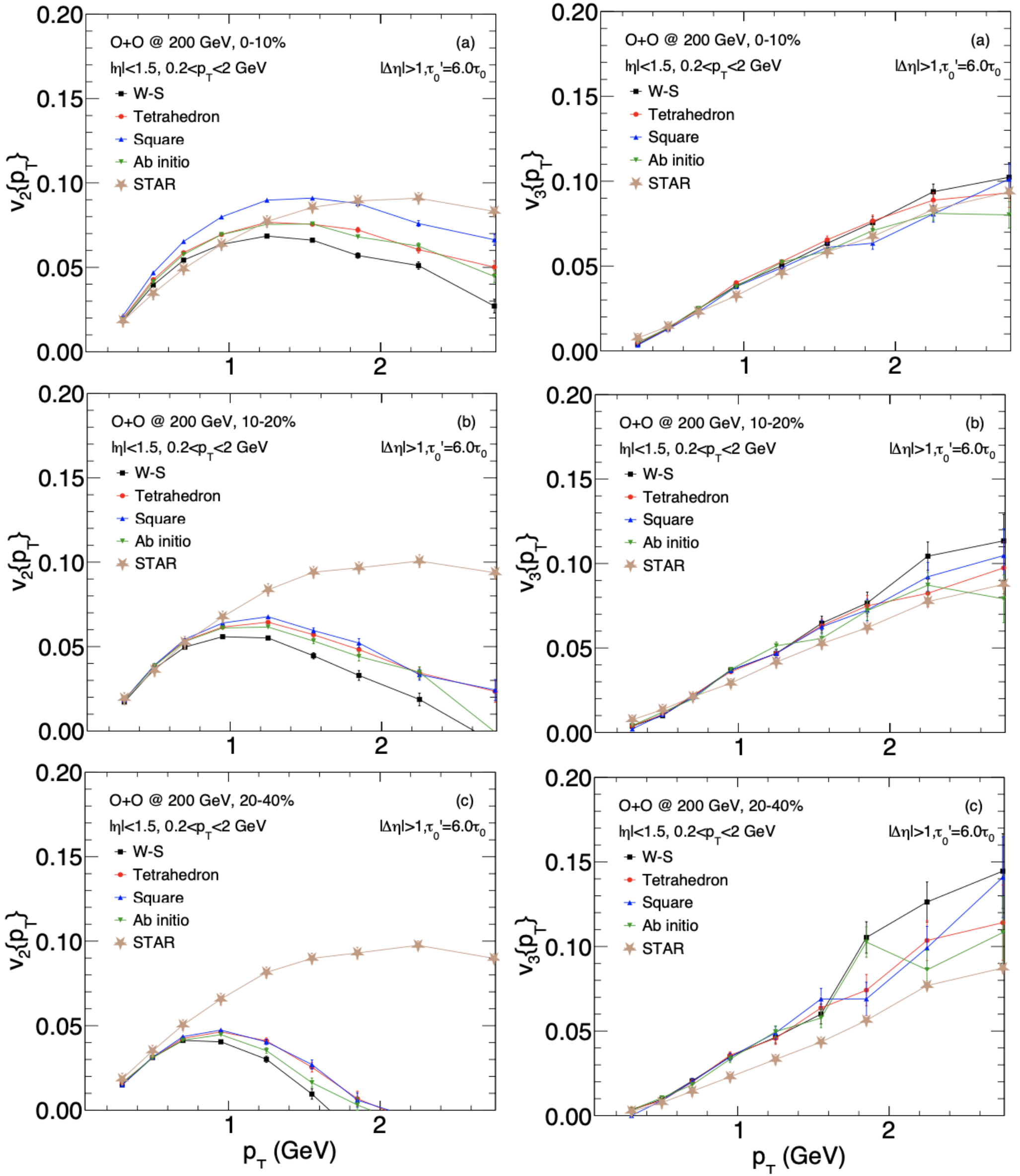

- $v_2(p_T)$ results are close to data at low p_T.
- $v_3(p_T)$ results are close to data.

v_2 & v_3 Results for ^{16}O+ ^{16}O in Improved AMPT

X.L. Zhao, Y. Zhou, et al., arXiv: 2404.09780

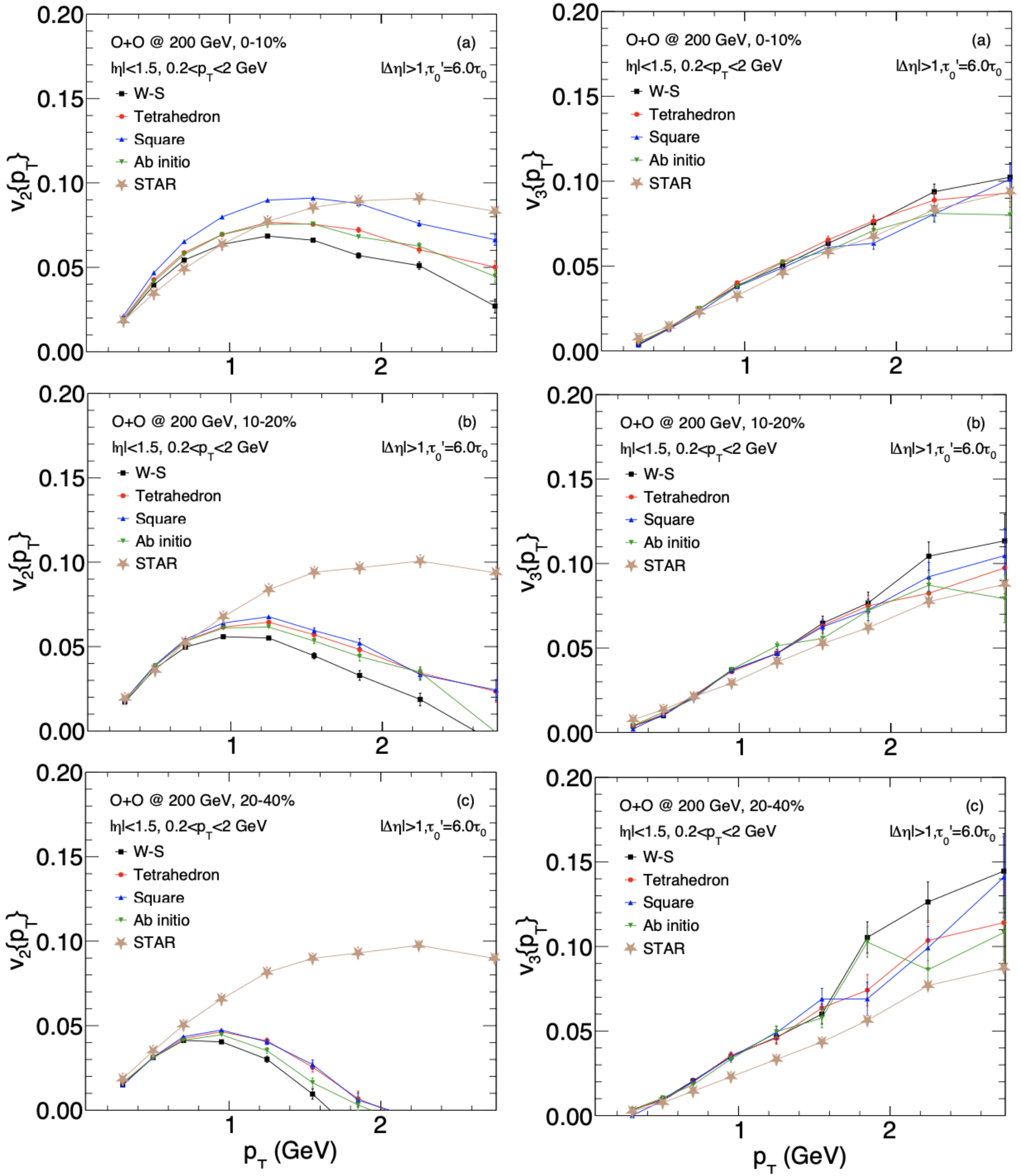

- $v_2(p_T)$ results are close to data at low p_T.
- $v_3(p_T)$ results are close to data.

- The effect of cluster structure is significant for v_2.
- The v_3 results are higher than data.

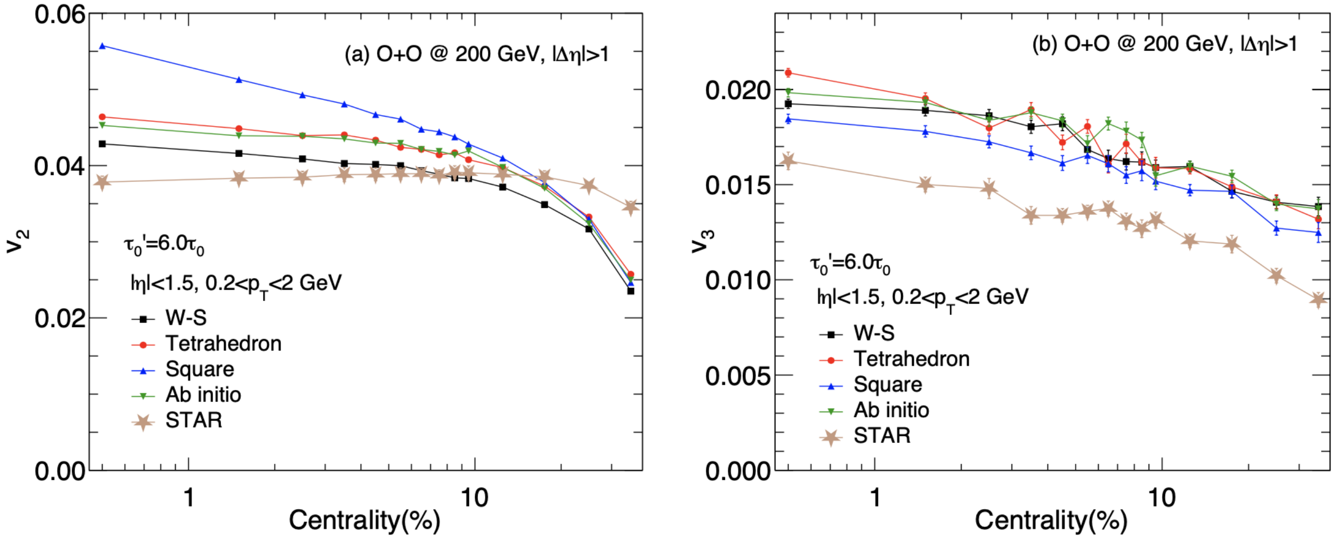

$\varepsilon_2\{4\}/\varepsilon_2\{2\}$& $v_2\{4\}/v_2\{2\}$ Results for $^{16}O+^{16}O$ in Improved AMPT

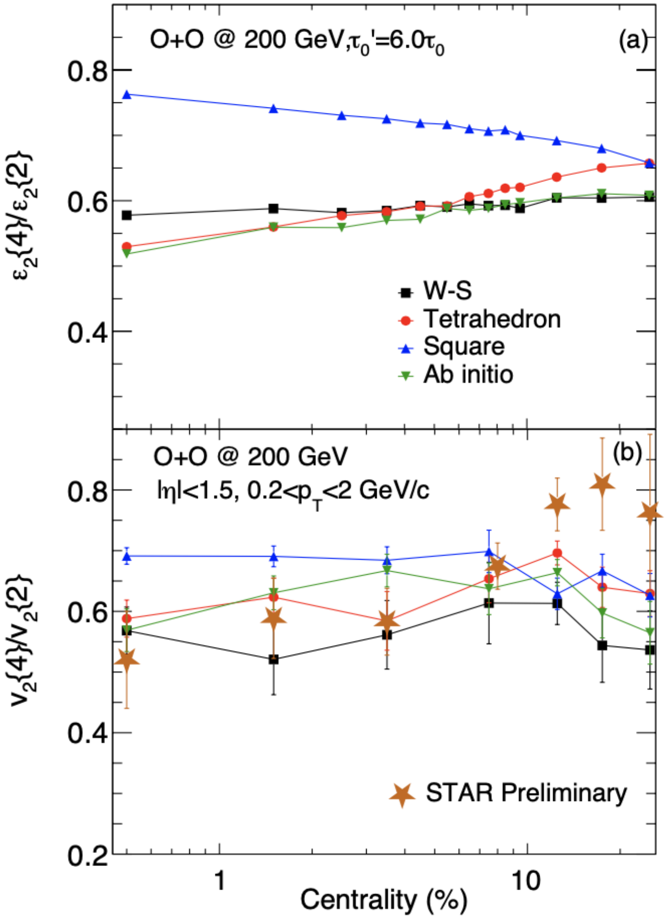

X.L. Zhao, Y. Zhou, et al., arXiv: 2404.09780

$$\varepsilon_2\{2\}^2 = \langle\varepsilon_2^2\rangle = \langle\varepsilon_2\rangle^2 + \sigma_{\varepsilon_2}^2$$

$$\varepsilon_2\{4\}^2 = (-\langle\varepsilon_2^4\rangle + 2\langle\varepsilon_2^2\rangle^2)^{1/2} \approx \langle\varepsilon_2\rangle^2 - \sigma_{\varepsilon_2}^2$$

- $\varepsilon_2\{4\}/\varepsilon_2\{2\}$ & $v_2\{4\}/v_2\{2\}$ results are consistent.
- Compared to the STAR on the $v_2\{4\}/v_2\{2\}$ ratio, the tetrahedron and *ab initio* cases give better descriptions of the STAR data.

$\varepsilon_2\{4\}/\varepsilon_2\{2\}$& $v_2\{4\}/v_2\{2\}$ Results for ^{16}O+ ^{16}O in Improved AMPT

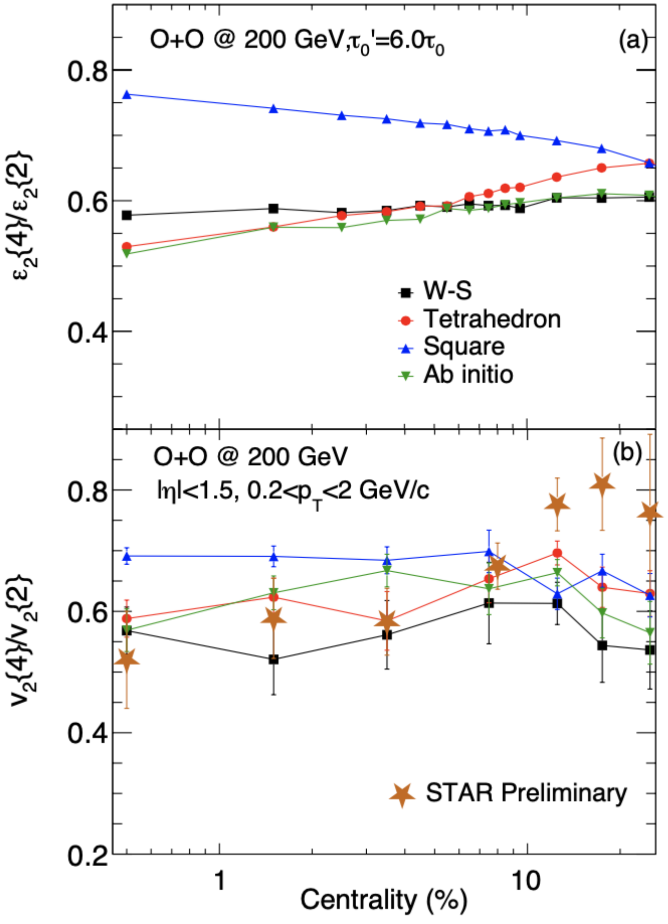

X.L. Zhao, Y. Zhou, et al., arXiv: 2404.09780

$$\varepsilon_2\{2\}^2 = \langle\varepsilon_2^2\rangle = \langle\varepsilon_2\rangle^2 + \sigma_{\varepsilon_2}^2$$

$$\varepsilon_2\{4\}^2 = (-\langle\varepsilon_2^4\rangle + 2\langle\varepsilon_2^2\rangle^2)^{1/2} \approx \langle\varepsilon_2\rangle^2 - \sigma_{\varepsilon_2}^2$$

- $\varepsilon_2\{4\}/\varepsilon_2\{2\}$ & $v_2\{4\}/v_2\{2\}$ results are consistent.
- Compared to the STAR on the $v_2\{4\}/v_2\{2\}$ ratio, the tetrahedron and *ab initio* cases give better descriptions of the STAR data.

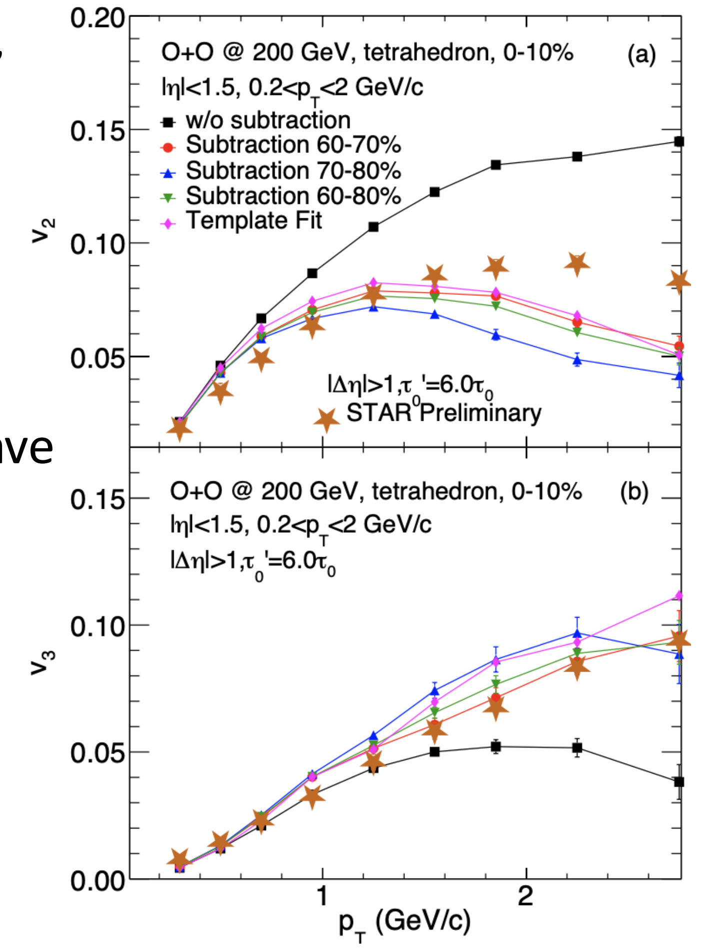

- The non-flow subtraction methods have little effect on v_2, especially on v_3.

$$\frac{dN^{\mathrm{pairs}}}{d\Delta\phi} \propto 1 + 2\sum_{n=1}^{\infty} v_n \cos(n\Delta\phi)$$

$$Y(\Delta\phi, p_{\mathrm{T}}^{\mathrm{trig}}) = c_0(1 + 2\sum_{n=1}^{n=4} c_n \cos(n\Delta\phi))$$

$$c_n^{\mathrm{sub}} = c_n - c_n^{\mathrm{non-flow}} = c_n^{\mathrm{cent}} - c_n^{\mathrm{peri}} \times f$$

Nuclear Structure for ^{16}O & ^{20}Ne in AMPT

1) New quark coalescence model
2) Improved heavy quark productions
3) Modern PDFs, nuclear shadowing and Local nuclear scaling

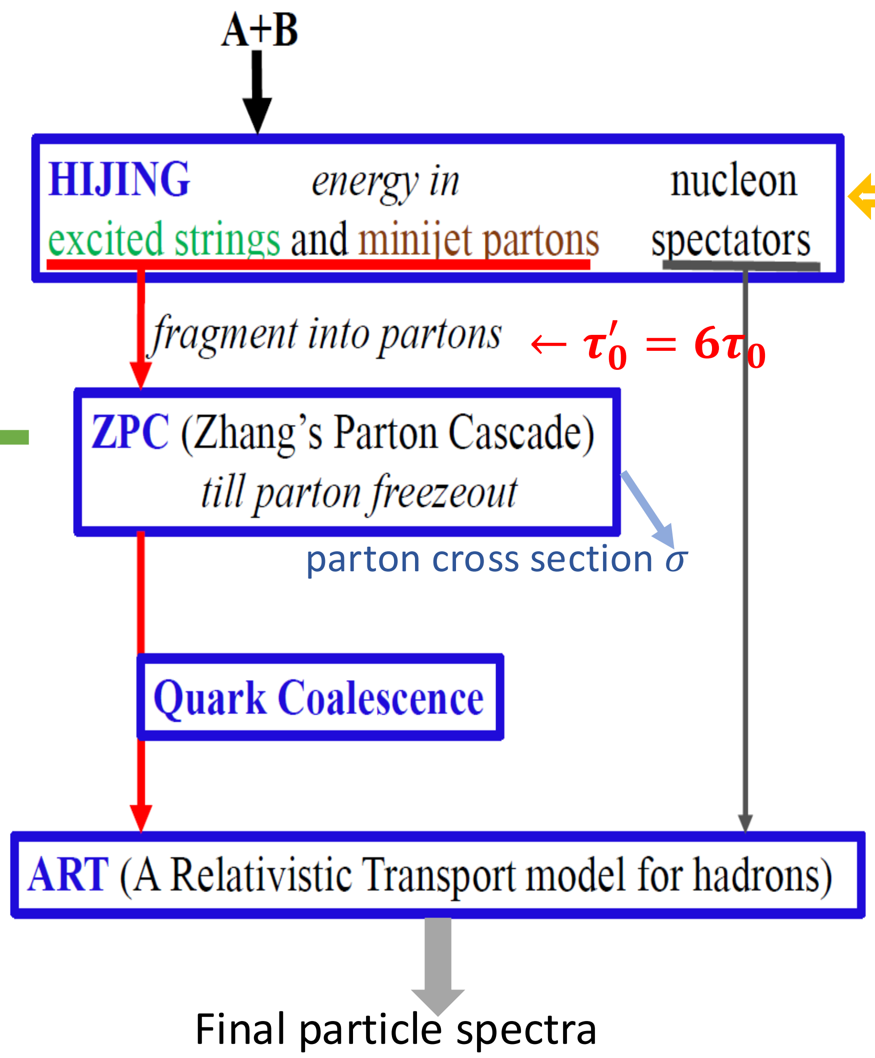

Giuliano Giacalone, et al. arXiv: 2402.05995

1. NLEFT (^{16}O & ^{20}Ne)

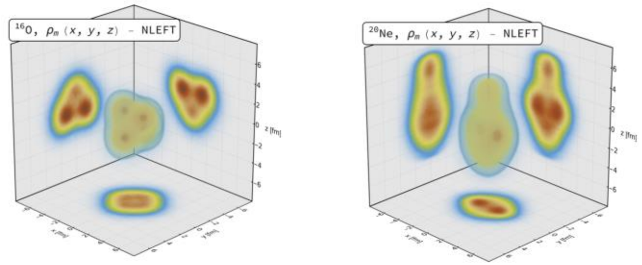

2. PGCM (^{16}O & ^{20}Ne)

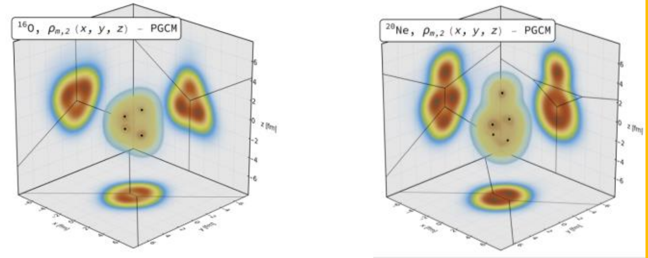

v_2 & v_3 Results for $^{16}O+^{16}O$ & $^{20}Ne+^{20}Ne$ in Improved AMPT

G. Giacalone, B. Bally, G. Nijs, D. Lee, B.N. Lu, W. van der Schee,, et al. arXiv: 2402.05995

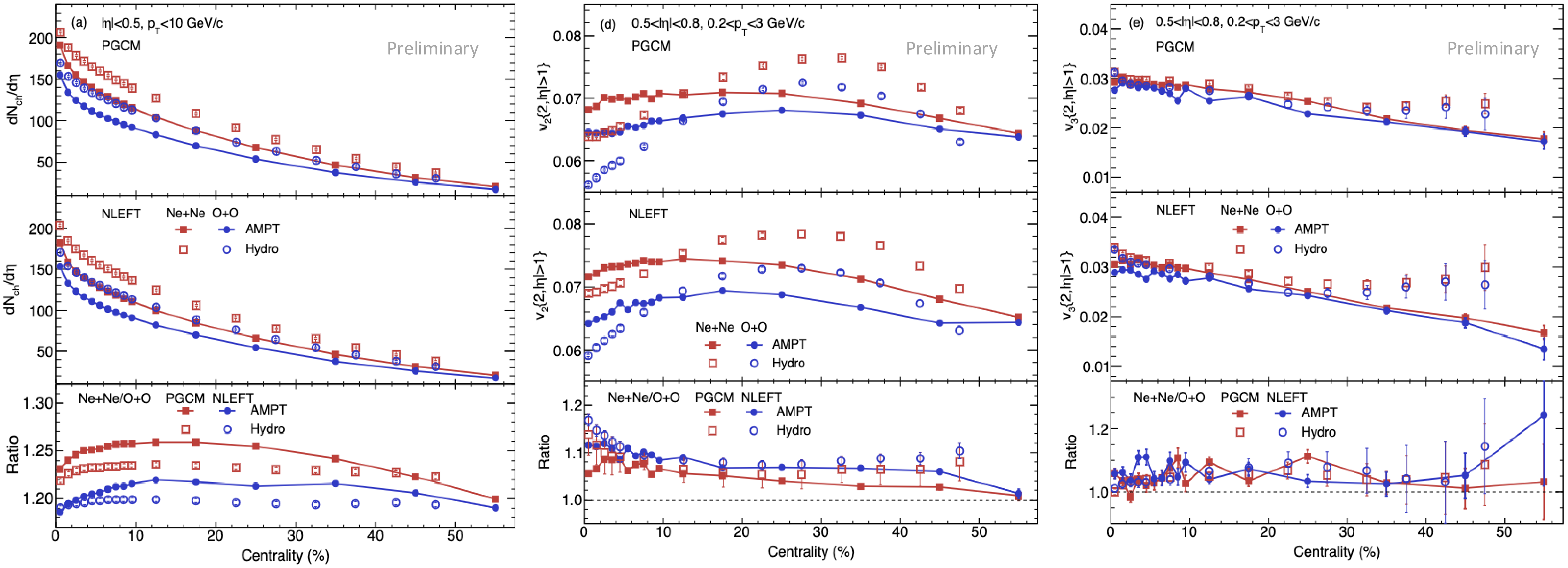

- ➢ Using the same initial nucleon distributions, AMPT has the different results with hydro.
- ➢ Some improvements are needed.

v_2 & v_3 Results for ^{16}O+^{16}O & ^{20}Ne+^{20}Ne in Improved AMPT

G. Giacalone, B. Bally, G. Nijs, D. Lee, B.N. Lu, W. van der Schee,, et al. arXiv: 2402.05995

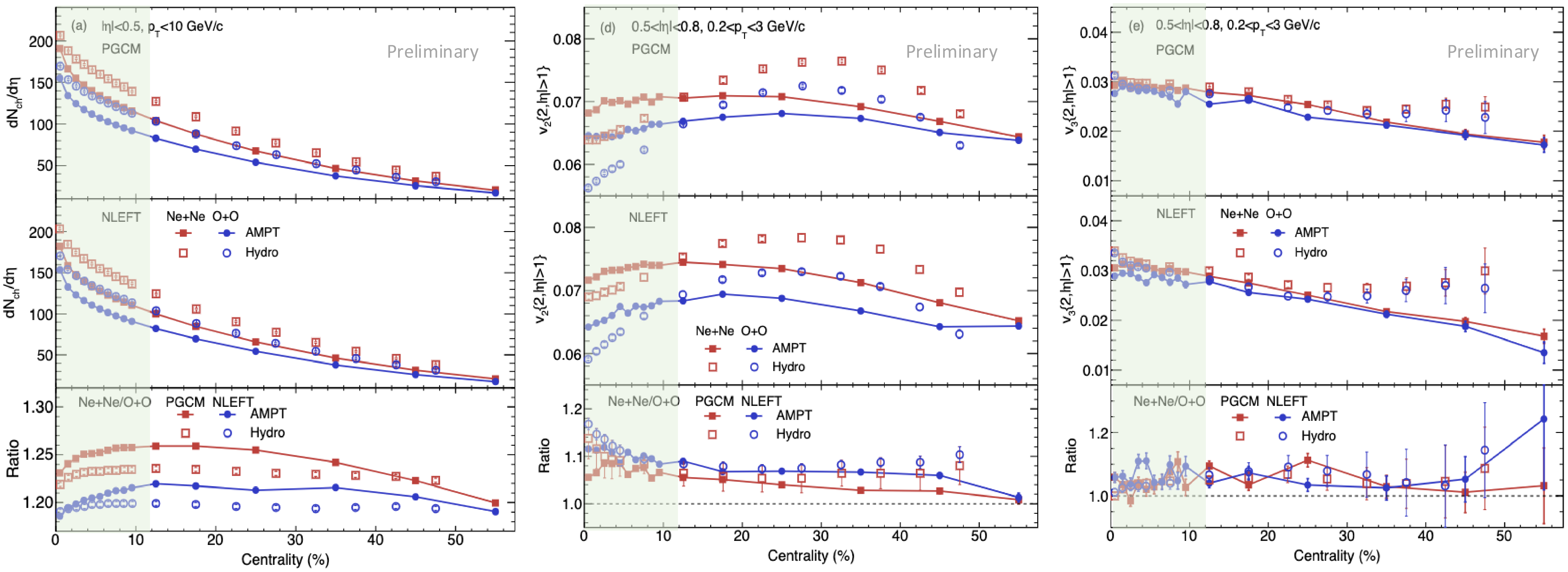

- Using the same initial nucleon distributions, AMPT has the different results with hydro.
- Some improvements are needed.

Problems for $^{16}O+^{16}O$ / $^{20}Ne+^{20}Ne$ in Improved AMPT

- **Same inputs**: initial nucleon distributions are consistent with hydro.
- **Different ε_2**: the initial condition is different from hydro.

To keep the same ε_2, 1) $\tau_0' = \tau_0$ for partons.

2) change the reduced thickness in AMPT.

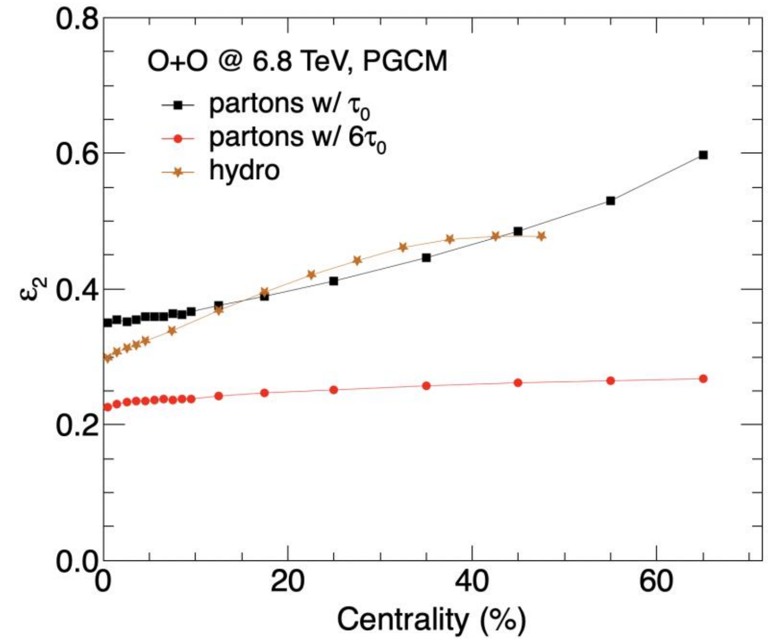

reduced thickness

$$f = T_R(p;\, T_A, T_B) \equiv \left(\frac{T_A^p + T_B^p}{2}\right)^{1/p}$$

$$T_R = \begin{cases} \max(T_A, T_B), & p \to +\infty \\ (T_A + T_B)/2, & p = +1 \text{ (arithmetic)} \\ \sqrt{T_A T_B}, & p = 0 \text{ (geometric)} \\ 2T_A T_B/(T_A + T_B), & p = -1 \text{ (harmonic)} \\ \min(T_A, T_B), & p \to -\infty. \end{cases}$$

PRC 92, 011901(R) (2015)

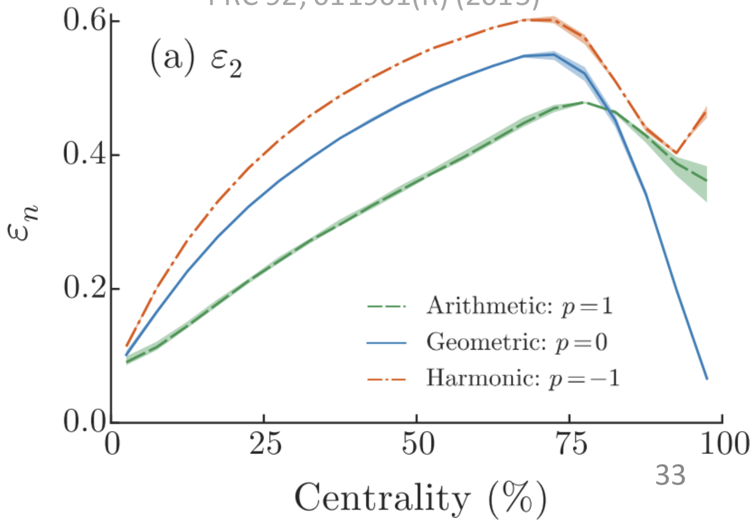

Problems for $^{16}O + ^{16}O$ / $^{20}Ne + ^{20}Ne$ in Improved AMPT

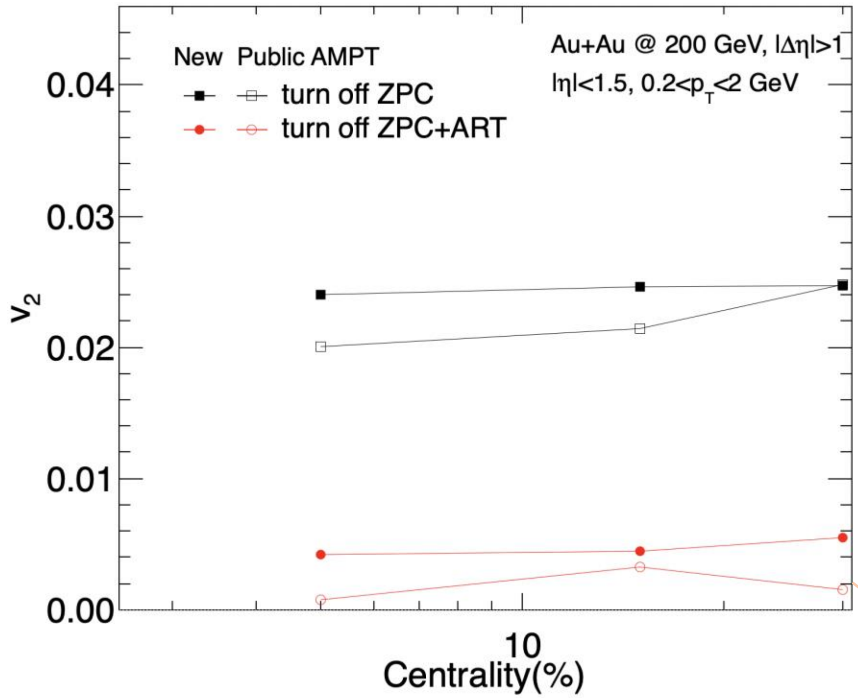

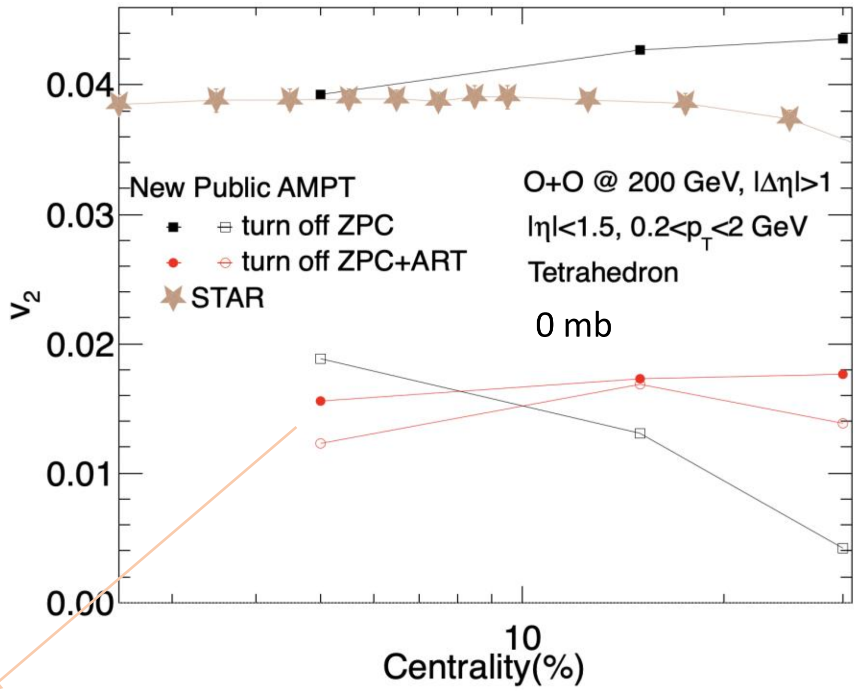

$v_2^2 < 0$

Problems for $^{16}O+^{16}O$ / $^{20}Ne+^{20}Ne$ in Improved AMPT

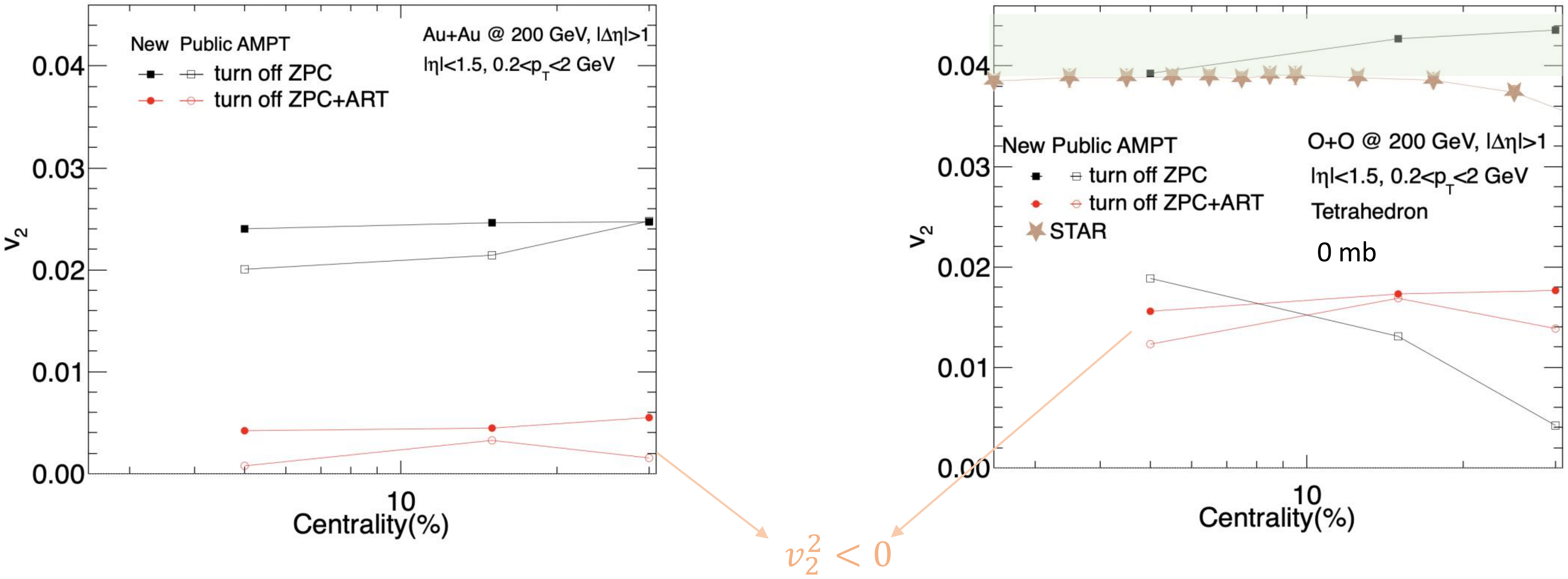

- For Au+Au collisions in public and improved AMPT, the hadronic effect of v_2 are almost zero.
- For O+O collisions in improved AMPT, the hadronic effect of v_2 is not zero.
- **Hadronic effects of v_2 are different in O+O & Au+Au collisions.**
- A simple method to solve this problem is the additional formation time for hadrons.

Summary & Outlook

- Improved AMPT roughly reproduce the STAR data for O+O collisions.
- Different nuclear structures have obviously effect on v_2 & v_3 in AMPT.
- The studies of O+O & Ne+Ne collisions help explore the limit of QGP collectivity.
- Studying the same collision system with AMPT and hydro helps us to understand the properties of the QGP in small system collisions. But, it is necessary to ensure that the same initial conditions are available.
- AMPT is especially suitable for studies of non-equilibrium dynamics
- Recent developments have made the model more versatile and accurate.

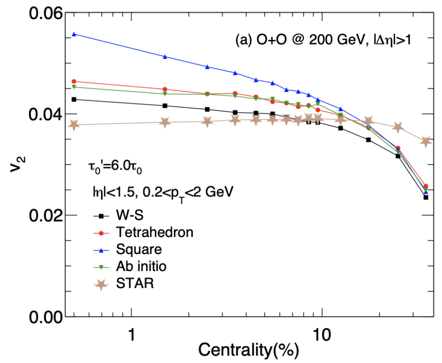

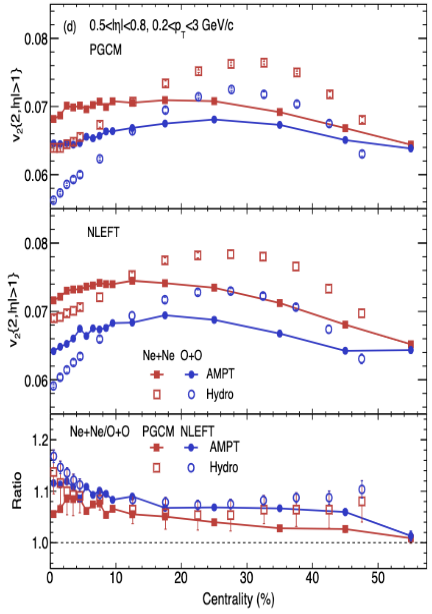

Summary & Outlook

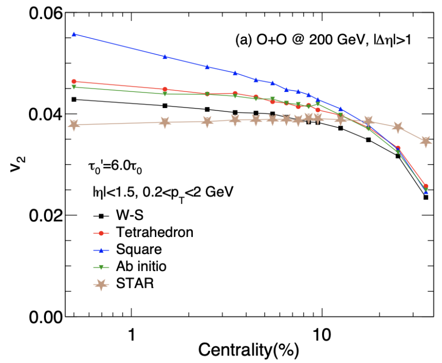

- Improved AMPT roughly reproduce the STAR data for O+O collisions.
- Different nuclear structures have obviously effect on v_2 & v_3 in AMPT.
- The studies of O+O & Ne+Ne collisions help explore the limit of QGP collectivity.
- Studying the same collision system with AMPT and hydro helps us to understand the properties of the QGP in small system collisions. But, it is necessary to ensure that the same initial conditions are available.
- AMPT is especially suitable for studies of non-equilibrium dynamics
- Recent developments have made the model more versatile and accurate.

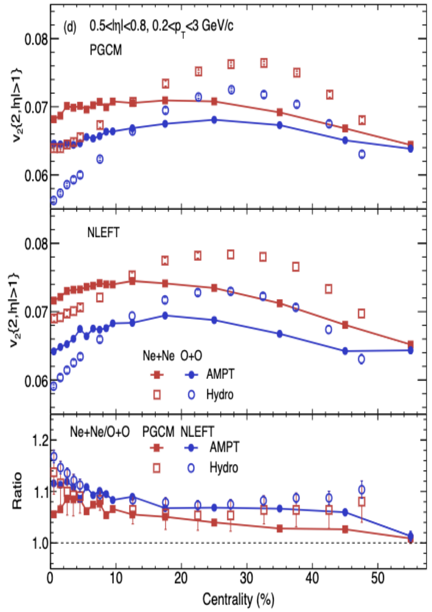

Thank you for your attention!

String Melting Version of A Multi-Phase Transport Model (AMPT)

- A transport model for non-equilibrium.

- AMPT is designed to be a self-contained kinetic description of nuclear collisions.
- Evolves the system from initial state to final observables.
- Automatically includes 3D productions of all flavours & conserved charges.
- Automatically includes non-equilibrium initial state & dynamics/evolution.

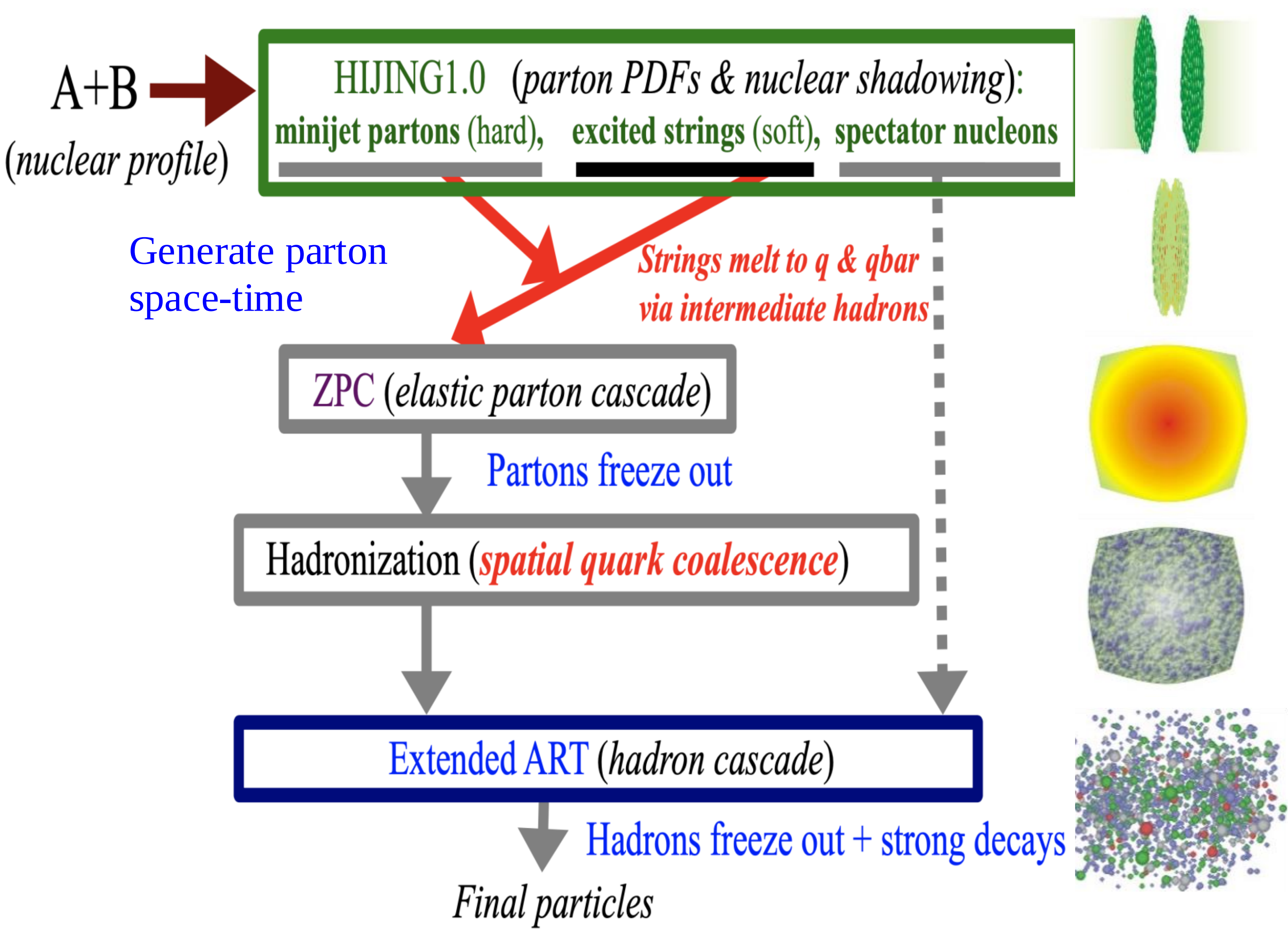

Z.W. Lin, Phys. Rev. C 72 (2005) 064901.

Additional Formation Time for Hadrons in Improved AMPT

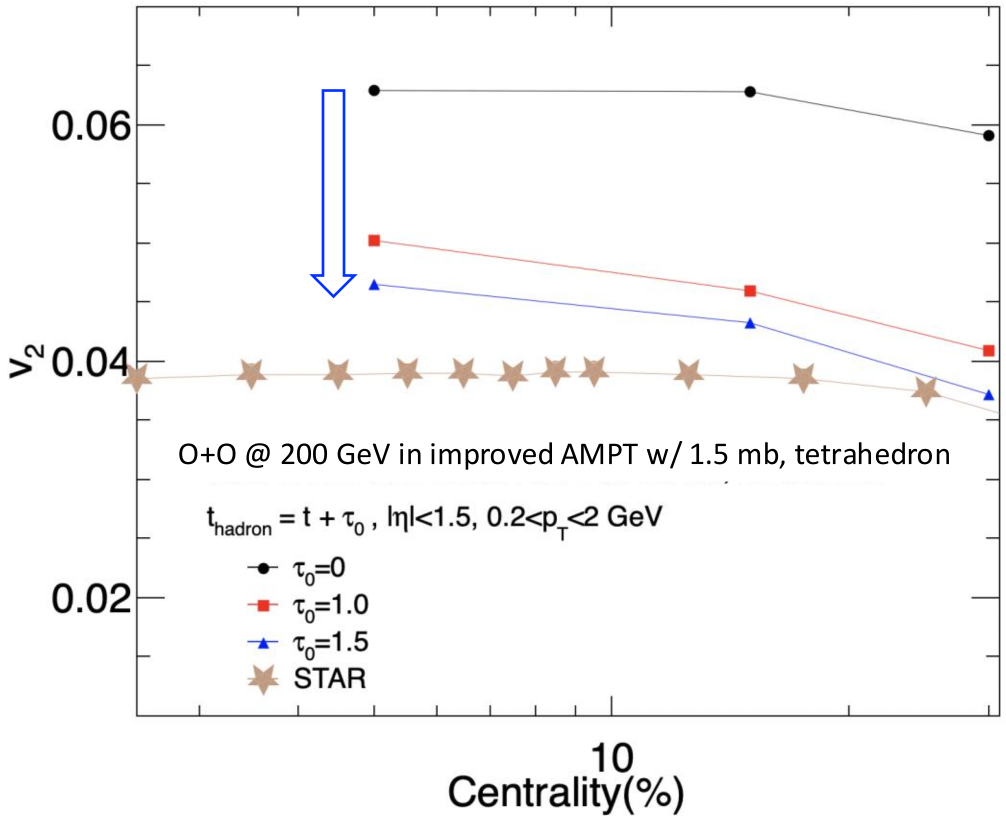

- ➢ An additional formation time for hadrons can solve the hadronic effects for O+O collisions.